Redox-State Dependent Ligand Exchange in Manganese-Based Oxidation Catalysis

Abdolahzadeh, Shaghayegh; de Boer, Johannes W.; Browne, Wesley R.

Published in:
European Journal of Inorganic Chemistry

DOI:
10.1002/ejic.201500134

Publication date:
2015

EurJIC European Journal of Inorganic Chemistry

ChemPubSoc Europe

MICROREVIEW

DOI:10.1002/ejic.201500134

Redox-State Dependent Ligand Exchange in Manganese-Based Oxidation Catalysis

CLUSTER ISSUE

Shaghayegh Abdolahzadeh,[a] Johannes W. de Boer,[b] and Wesley R. Browne*[a]

Keywords: Redox chemistry / Oxidation / Peroxides / Manganese / Coordination modes

Manganese-based oxidation catalysis plays a central role both in nature, in the oxidation of water in photosystem II (PSII) and the control of reactive oxygen species, as well as in chemical processes, in the oxidation of organic substrates and bleaching applications. The focus of this review is on efforts made to explore and elucidate the redox-dependent coordination chemistry of these manganese-based systems in solution and the mechanisms by which their catalytic redox reactions proceed. We also examine the behaviour and activity of complexes that have been developed and used as models for the active sites of the corresponding enzymes, or used as catalysts in the oxidation of organic substrates. Given the current concern over the environmental and economic impact of chemical processes, manganese catalysts that use H_2O_2 as oxidant are the primary focus of this review.

1. Introduction

Oxidation catalysis, especially that involving oxygen, plays a central role in both biochemical[1] and industrial processes.[2,3] The oxidation of organic substrates to highly functionalized organic compounds, for example, oxidation of olefins to the corresponding diols or epoxides,[4] alcohols

[a] Stratingh Institute for Chemistry, Faculty of Mathematics and Natural Sciences, University of Groningen, Nijenborgh 4, 9747 AG Groningen, The Netherlands
E-mail: w.r.browne@rug.nl
http://www.rug.nl/research/molecular-inorganic-chemistry/browne
[b] Chemsenti Ltd., BioPartner Center Leiden, Galileiweg 8, 2333 BD Leiden, The Netherlands

Shaghayegh Abdolahzadeh received her BSc in Pure Chemistry from Shahid Beheshti University, Tehran, and completed her MSc in Analytical Chemistry in the Center of Excellence in Electrochemistry, Faculty of Chemistry, University of Tehran, Iran. She subsequently moved to the University of Groningen, The Netherlands, to take up a PhD position in the group of Prof. Browne. Her research interests include the mechanisms by which manganese catalysts engage in bleaching and alkene oxidation and in the development of novel analytical techniques for reaction monitoring.

Johannes W. de Boer received his PhD in Chemistry (2008) from the University of Groningen, The Netherlands, under the guidance of Prof. Ben L. Feringa and Dr Ronald Hage and was awarded the Backer Prize from the Royal Dutch Chemical Society for his thesis on manganese catalyzed cis-dihydroxylation and epoxidation reactions. Since 2007 he has been working for Rahu Catalytics, Catexel and Chemsenti (which are spin-outs from Unilever) as Research Principal. His current research interests include the development of new oxidation catalysts and processes for a wide variety of (industrial) applications, focusing on manganese and iron catalyzed activation of hydrogen peroxide and oxygen.

Wesley R. Browne received his BSc in Pure and Applied Chemistry and PhD in Chemistry (2002), focused on ruthenium polypyridyl photochemistry and photophysics, from Dublin City University, Dublin, Ireland, under the supervision of Prof J. G. Vos and for which he was awarded the Young Chemists Award from the Royal Irish Academy. After Postdoctoral positions at Queens University Belfast, under Prof. J. J. McGarvey and subsequently at the University of Groningen under Prof. B. L. Feringa, he was appointed as assistant Professor at the Stratingh Institute for Chemistry in 2008. In 2007, he was awarded a VIDI Innovational research award from The Netherlands Organisation for Science (NWO) and, in 2011, an ERC Starting Investigator Grant by the European Research Council. In 2013 he was appointed as Associate Professor and in 2015 as Chair of Molecular Inorganic Chemistry at the University of Groningen. His research interests include electrochemistry and Raman spectroscopy and microscopy applied in particular to oxidation catalysis.

to aldehydes, ketones or carboxylic acids, the oxidation of alkanes and the bleaching of stains and raw materials are of enormous economic importance.[5–8] Among the many oxidants available, H_2O_2 and O_2 are preferred because they are inexpensive, readily available, have a high oxygen content and are environmentally benign, with usually only water formed as a waste product.[9] Although these oxidants are appealing for applications in synthetic chemistry and bleaching, their intrinsic activity is kinetically limited under ambient conditions. This is partly because the reaction of dioxygen ($^3O_2$) with closed-shell organic compounds is spin-forbidden, despite being a highly exergonic reaction, and proceeds through the formation of free radical intermediates.[10]

The chemistry of oxygen is dominated by its relatively unreactive forms: water (H_2O, the fully reduced state) and dioxygen ($^3O_2$, the fully oxidised state),[11] whereas the intermediate forms, i.e., the hydroxyl radical ($OH^{\cdot}$), hydrogen peroxide (H_2O_2) and the superoxide radical ($O_2^{\cdot-}$), are highly reactive. Nature has evolved numerous enzymes based on a wide range of transition metals,[1] including iron, copper and manganese, to harness the remarkably rich redox chemistry of oxygen. The paramount examples are, almost certainly, the oxidation of water to dioxygen by the oxygen evolving complex (OEC) of photosystem II (PSII),[12–18] and the disproportionation of H_2O_2 and superoxide by catalases,[19,20] and superoxide dismutases,[21–23] respectively, which mitigate the oxidative stress placed on living cells by reactive oxygen species (ROS). Biological systems are able to activate dioxygen for controlled chemical synthesis through electron- and proton-transfer at the transition-metal-based catalytic sites in enzymes. Achieving such control in synthetic systems, however, requires an understanding of the redox-controlled coordination chemistry of metal complexes.

The presence of manganese at the active sites of many enzymes,[24] which are responsible for these key biochemical processes, has stimulated the synthesis and characterization of manganese complexes[12,25,26,27–29] to mimic the active sites functionally and/or structurally. The coordination chemistry of manganese is complex given the ready accessibility of a wide range of oxidation states that are stable under ambient conditions (Mn^{II} to Mn^{VII}), and is complicated further by its propensity to form well-defined mono- and multi-nuclear complexes. For dinuclear systems, depending on the ligands present, all oxidation states from $Mn^{II}Mn^{II}$ to $Mn^{IV}Mn^{IV}$ have been observed in aqueous media. μ-Oxido and μ-carboxylato bridged multinuclear manganese complexes (especially in the Mn^{III}, Mn^{III} and Mn^{IV} oxidation states) are important classes in regard to their redox chemistry and the occurrence of these structural motifs in the active sites of various manganese-containing redox enzymes. Furthermore, such complexes are ubiquitous with respect to their application in oxidation catalysis.

Direct spectroscopic data on the structure of the reactive intermediates formed by manganese complexes is, however, often of limited availability and therefore our mechanistic understanding is based largely on inferences drawn from catalytic activity; in particular, the analysis of reaction products, reactivity with various terminal oxidants, and the effect of additives on catalyst performance, etc.[5] In addition, the lability of manganese complexes when in low oxidation states, in particular Mn^{II}, increases the challenges faced in speciation analysis, especially in aqueous solutions.

The paradigm in manganese oxidation catalysis is by-and-large that Mn^{IV} and Mn^{V}[30–34] mononuclear complexes are the reactive intermediates that engage in substrate oxygenation.[35–38] However, in cases where such species have been observed, they usually reinforce Halpern's premise that if a species can be observed in a catalytic system, then it is at most a resting state. Furthermore, the widespread use and variety of, so-called, additives in manganese oxidation catalysis reflects the complexity in the roles they play, over and above their roles as potential ligands.

In this review, the solution chemistry of manganese-based complexes of interest to oxidation catalysis in both biological as well as chemical processes will be discussed. The focus is on understanding the mechanisms by which the manganese catalysts operate; in particular, those that were developed and used as model compounds for the active sites of the corresponding enzymes or used as catalysts in the oxidation of organic substrates. The interplay between changes in redox state and coordination chemistry will be highlighted as well as how these processes are affected by the presence of oxygen in its various forms (i.e., water, hydroxyl radical, hydrogen peroxide, superoxide and/or dioxygen) and other agents present in solution (e.g., co-catalytic additives). The importance of a diverse range of experimental parameters in controlling the reactivity and selectivity observed in the preparation of fine chemicals with manganese catalysed oxidations has been discussed in depth elsewhere.[5,6] In addition, with respect to increased attention to the environmental and economic impact of chemical processes, systems that use H_2O_2 as an oxidant will be the primary focus of this review, rather than those in which oxidants such as peracids, hypochlorite, Oxone etc. are employed.[39–42]

The goal of this review is to survey the approaches that have been taken to understand, first and foremost, the coordination chemistry of manganese-based catalysts in solution and, secondly, to draw correlations with the behaviour and activity of complexes under reaction conditions. First, the redox-dependent exchange of two ligands that are ubiquitous in manganese complexes, i.e., carboxylato and oxido ligands, will be discussed. Model complexes of three classes of manganese-containing metalloenzymes, which are responsible for the catalytic oxidation of water, the disproportionation of H_2O_2 and the dismutation of superoxide, respectively, are discussed. This is followed by selected examples of reactions involving manganese-containing catalysts employing H_2O_2 for the oxidation of substrates in organic and in aqueous media in which insight into mechanisms has been gained.

The transient nature of the species that are directly responsible for the oxidation of substrates makes their spec-

troscopic observation highly challenging, if not, in many cases impossible. Nevertheless, spectroscopic and electrochemical methods have been essential in elucidating overall reaction mechanisms, especially where a multi-technique approach is applied under catalytically relevant conditions. Indeed, although UV/Vis absorption spectroscopy is perhaps the most widely applied technique to study manganese complexes, FTIR absorption,[43] Raman[44] and, especially, resonance Raman,[45–49] and electron spin resonance (ESR) spectroscopy,[50,51] have proven invaluable in probing the structures of manganese complexes in solution. NMR spectroscopy[52] is, despite the paramagnetic nature of many manganese complexes, also useful in their study because many bi- and multi-nuclear complexes show strong antiferromagnetic interactions, in particular $Mn^{III}Mn^{III}$ and $Mn^{IV}Mn^{IV}$ complexes.[53] In addition, X-ray based techniques, over and above X-ray crystallography, although not yet widely accessible, are having an increased impact in the study of manganese complexes. Indeed, X-ray absorption techniques (e.g., EXAFS, XANES etc.)[54] provide key tools in determining electron density, and thus oxidation state, at the metal centres in both synthetic complexes and enzymes.[55]

In terms of developing our mechanistic understanding of the chemistry of redox-active manganese complexes, cyclic voltammetry (CV)[56–58] and, to a lesser extent, spectroelectrochemistry,[59,60] in which a sample undergoing electrolysis is characterised in situ with a spectroscopic technique (e.g., UV/Vis, FTIR, Raman or EPR spectroscopy), have proven invaluable because they enable access to and characterisation of often highly reactive species. Similarly, electrospray ionisation mass spectrometry (ESI-MS),[61–65] is perhaps the most important of the mass spectrometric techniques with regard to the characterisation of manganese complexes, especially because reaction mixtures can be sampled directly. Mass spectrometry has its own set of limitations that are especially important in the present context. Complexes in lower oxidation states, which are highly labile, present problems because of the potential for ligand exchange and redox reactions to occur due to the (high) voltages used and the difficulty in controlling pH and dilution, and/or the high temperatures encountered within the mass spectrometer. For example, in the case of more kinetically stable complexes, i.e., in Mn^{III} and Mn^{IV} oxidation states, facile reduction coupled with ligand exchange can easily occur, giving rise to erroneous impressions of the distribution of species present in solution. Hence, drawing firm conclusions with regard to speciation from ESI-MS data is highly challenging. Recent innovations in cryo-ESI-MS,[66] however, should go a considerable way to improving the applicability of the technique in this field.

2. Exchange of Acetato and Oxido Ligands in Multinuclear Manganese Complexes

Over recent decades, synthetic manganese complexes bearing oxido and carboxylato ligands have been of particular interest in efforts to mimic the functional and spectroscopic properties of bioinorganic complexes such as the water oxidation complex (WOC) in photosystem II (PSII)[67] and manganese superoxide dismutases[68] and catalases.[69] A key aspect of the functionality of these biological systems is that redox changes can affect the coordination mode, in particular binding and dissociation of carboxylato and oxido ligands.

In this section, the focus will rest on ligand exchange processes and the redox dependence of both the rate of ligand exchange and on changes in coordination that accompany changes in redox state. Several examples will be discussed in which ligand exchange processes have been studied and, in particular, how changes in redox state can drive changes in coordination mode.

2.1. The Water Splitting Centre of Photosystem II

Water oxidation, which is a key reaction in nature, is perhaps the paradigm example of the importance of coupling changes in redox state with changes in coordination environment. It is remarkable that such a complex process can be carried out at low overpotential by the $CaMn_4$ cluster that lies at the heart of the oxygen-evolving complex (OEC) of photosystem II.[70,71] In the OEC, the catalytic tetranuclear Mn_4 core cycles through five oxidation states to accumulate sufficient redox potential and equivalents to oxidise water ($2\ H_2O \rightarrow O_2 + 4\ H^+ + 4\ e^-$). Despite being the focus of intense study for decades, only recently was the detailed structure of the OEC revealed by X-ray crystallography.[72] It has been, however, the lack of crystallographic evidence for the structure of the OEC that has stimulated the synthesis of a wide range of structural and, more recently, functional models. Although the complete cycle is still not clear in detail, the model for its function as described by Kok et al.[73] is widely accepted and involves a cycle comprised of five flash-induced transitions between the so-called S-states, denoted as S_0–S_4, with the S_0 state being the most reduced and the S_4 state the most oxidised. The $S_1 \rightarrow S_2$ transition is considered as primarily an oxidation step, i.e. without an accompanying change in the coordination environment, whereas the other transitions between the S-states involve removal of an electron and proton from the OEC.[74] The S_4 state decays spontaneously to recover the S_0 state with concomitant release of dioxygen. It is clear that the structural changes, i.e. changes in the coordination of the ligands bound to the manganese ions, that accompany changes in redox state, are central to the operation of the OEC.[75]

Spectroscopic, structural and electrochemical data garnered over the last decades from synthetic manganese complexes[32,76,77] have provided an important basis to understand the highly complex chemistry of the OEC.[12,25,26,78] Generally, the primary focus has been on structural mimicry, however, and several synthetic complexes have indeed been shown to be also able to oxidise water.[77e,77g,77j,79] The first report on water oxidation by a

synthetic manganese complex, i.e., $[Mn^{III}Mn^{IV}(\mu\text{-}O)_2(terpy)_2(H_2O)_2]^{3+}$, in aqueous solution by Crabtree, Brudvig and co-workers has stimulated enormous interest in this area.[32]

2.2. Rate of Exchange of Acetato, Aquo and Oxido Ligands in Multinuclear Manganese Complexes

A highly accessible method to assess the lability of ligands is to use ^{18}O-labelled water to monitor exchange by ESI-MS. Tagore et al.[34] have employed ESI-MS to determine the rates of μ-oxido exchange in acetonitrile, in the presence of trace water, for several bis-μ-oxido dimanganese complexes (Figure 1).

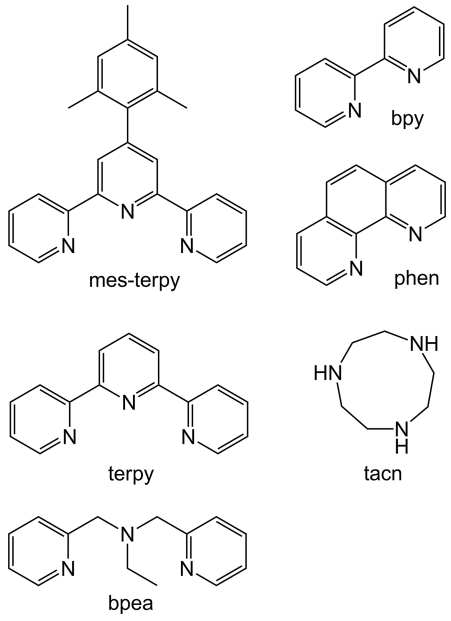

Figure 1. Ligands used in complexes **1**–**6**. $[(mes\text{-}terpy)_2Mn^{III}Mn^{IV}(\mu\text{-}O)_2(H_2O)_2](NO_3)_3$ (**1**, mes-terpy = 4′-mesityl-2,2′:6′,2′′-terpyridine), $[(bpy)_4Mn^{III}Mn^{IV}(\mu\text{-}O)_2](ClO_4)_3$ (**2**, bpy = 2,2′-bipyridine), $[(phen)_4Mn^{III}Mn^{IV}(\mu\text{-}O)_2](ClO_4)_3$ (**3**, phen = 1,10-phenanthroline), $[(bpea)_2Mn^{III}Mn^{IV}(\mu\text{-}O)_2(\mu\text{-}OAc)](ClO_4)_2$ (**4**, bpea = bis(2-pyridyl)ethylamine), $[(bpea)_2\ Mn^{IV}Mn^{IV}(\mu\text{-}O)_2(\mu\text{-}OAc)](ClO_4)_3$ (**4ox**), $[(terpy)_4Mn_4{}^{IV/IV/IV/IV}(\mu\text{-}O)_5(H_2O)_2](ClO_4)_6$ (**5**, terpy = 2,2′:6′,2′′-terpyridine), and $[(tacn)_4Mn_4{}^{IV/IV/IV/IV}(\mu\text{-}O)_6]Br_{3.5}(OH)_{0.5}\cdot 6H_2O$ (**6**, tacn = 1,4,7-triazacyclononane).

The exchange of the μ-oxido ligands in **2** and **3** with $H_2{}^{18}O$ was originally reported by Cooper and Calvin to occur only at high temperatures in aqueous solutions.[80] In acetonitrile with trace water, however, Tagore et al.[34] noted that exchange was as rapid as for the other complexes, albeit with an uncertainty due to the inability to observe the intact complexes by ESI-MS. The rate of the exchange of μ-OAc bridges with CD_3CO_2D for complexes **4** and **4ox**, which is of relevance to the reported inhibition of PSII by acetate,[81–85] is much higher than that of μ-O exchange. Comparison of the rate constants for ligand exchange indicates that μ-O exchange for Mn^{IV} complexes is slower than for Mn^{III} complexes and also slower than for a manganese centre that can switch between the Mn^{IV} and Mn^{III} oxidation states more rapidly than the rate of exchange. This difference in exchange rate was rationalised by the Jahn–Teller distortion present in a high-spin octahedral Mn^{III} (d^4) ion that is absent in an octahedral Mn^{IV} (d^3) ion. The availability of a labile coordination site also serves to enhance the rate of exchange of μ-oxido ligands. Notably, tetranuclear Mn^{IV} complexes **5** and **6** showed no evidence of exchange even over extended periods.

The mechanism of μ-O exchange in **1** and **3**, i.e., with and without terminal water-binding sites, respectively, was explored in further detail by Tagore et al.[86] The order in respect to complex is 1 in both cases, excluding bimolecular reactions, however, the order in $H_2{}^{18}O$ for the μ-O exchange was 1 and <1 for **1** and **3**, respectively. Addition of a Brønsted acid, such as HNO_3 or $HClO_4$ to **1** and **3**, respectively, increased the rate of μ-O exchange in acetonitrile for **1** and decreased it for **3**, indicating a difference in the mechanisms for exchange.

Addition of excess phen ligand decreased exchange rates and indicated that phen dissociation is important in the case of **3**, whereas dissociation of the mes–terpy in **1**, if it is necessary, has no effect on the exchange rate. DFT[87] calculations indicated that the bis-hydroxido form was less stable than the μ-oxido bridged form. The proposed mechanism of exchange in **1** (Scheme 1) involves protonation of the μ-O bridge by the water coordinated to the Mn^{IV} ion, which is more acidic. Based on the pK_a of the complex, reported oxido-exchange in aluminium–oxido clusters,[88] and bridge opening in manganese dimers due to protonation,[80,89,90] protonation followed by bridge opening is likely to be energetically favourable for **1**. In the case of **3**, dissociation of phen, which is followed by coordination of water, occurs prior to exchange of the μ-O bridge. Deprotonation of the water *trans* to the μ-oxido bridge was proposed to increase the sigma donor strength of the hydroxido ligand.

The absolute $^{16/18}O$ isotope exchange rates determined for **1** may provide insight into empirical data for the KIEs observed in various steps and states of the OEC.[91] The exchange rates measured for the S_0, S_2, and S_3 states of the OEC are ca. 800–4000 times greater than for **1** and are considered to be due to μ-O exchange. However, the μ-O exchange rate for **1** approaches (ca. 8 times slower) the slow exchange rate in the S_1 state of the OEC. The absence of terminal water-binding sites inhibits μ-O exchange in the S_1 state,[34] and dissociation of chelating ligands is therefore necessary for μ-O exchange when terminal water-binding sites are unavailable.

In the case of carboxylato bridged complexes based on the tmtacn ligand (1,4,7-trimethyl-1,4,7-triazacyclononane), e.g., $[Mn^{III}Mn^{III}(\mu\text{-}{}^{16}O)(\mu\text{-}CH_3CO_2)_2(tmtacn)_2]^{2+}$ (**7**), de Boer et al.,[92] have shown by ESI-MS that the rate of exchange of the μ-O bridge is dependent on the substituent on the carboxylato ligands. For example, whereas for **7** in $CH_3CN/H_2{}^{18}O$ (9:1), μ-O equilibration was complete within 8 min, for $[Mn^{III}Mn^{III}(\mu\text{-}{}^{16}O)(\mu\text{-}2,6\text{-}dichlorobenzoate)_2(tmtacn)_2]^{2+}$ (**8**) equilibration was complete

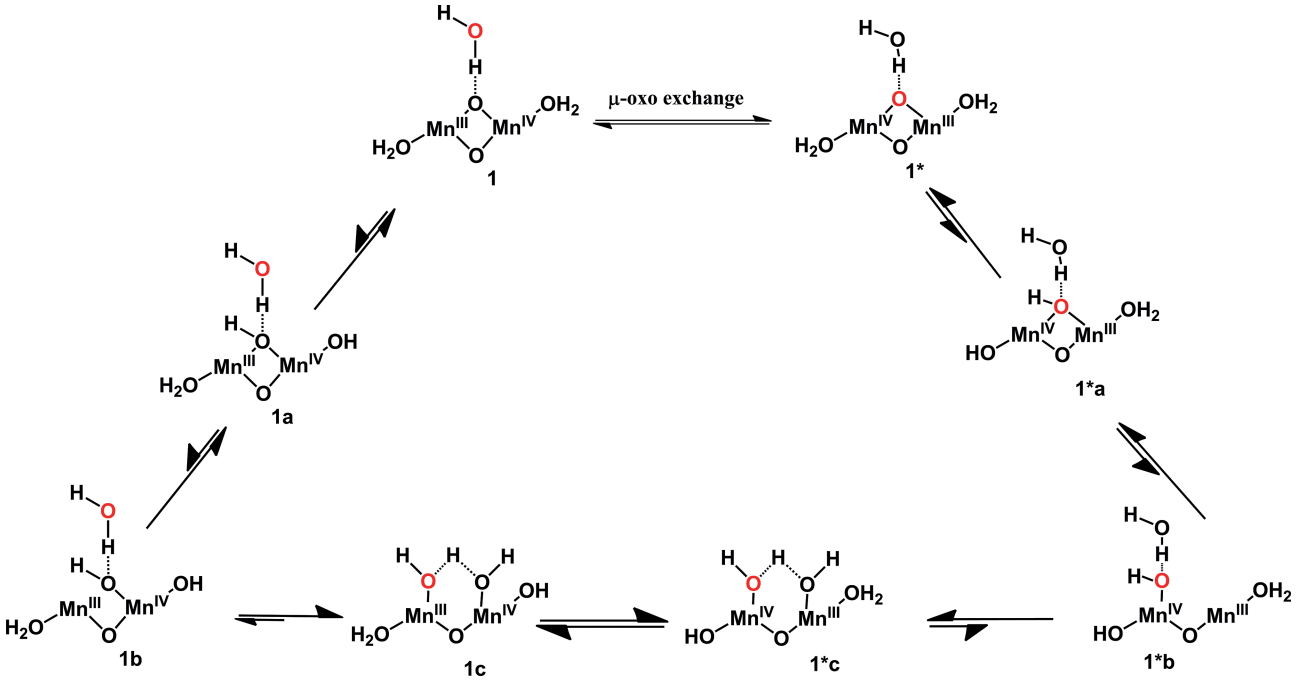

Scheme 1. Proposed mechanism of μ-O exchange in **1**, involving sequential oxido-bridge opening and coordination of labelled water.[86]

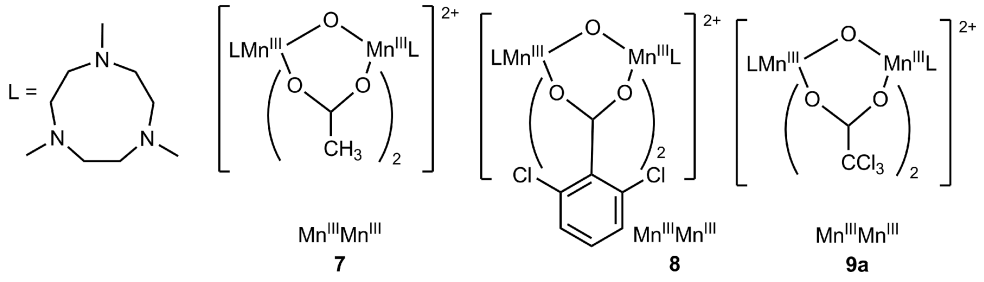

Figure 2. Structure of complexes **7**, **8** and **9a** based on the ligand tmtacn.

within 4 min and within 1 min for $[Mn^{III}Mn^{III}(\mu\text{-}^{16}O)(\mu\text{-}CCl_3CO_2)_2(tmtacn)_2]^{2+}$ (**9a**) (Figure 2).

The likely pathway for exchange of the μ-oxido bridges is associative, with opening of the μ-oxido bridge followed by coordination by $H_2{}^{18}O$ and subsequent closing of the μ-oxido bridge. Hence, the increase in the rate of μ-oxido exchange is likely to be due to the increase in the tendency for the μ-oxido bridge to open, which allows $H_2{}^{18}O$ to coordinate and facilitates exchange of other ligands through associative mechanisms.

2.3. Redox-State Dependent Exchange of Acetato, Aquo and Oxido Ligands in Multinuclear Manganese Complexes

The relation between manganese oxidation state and carboxylato stretching bands of monodentate coordinated carboxylates was studied by Berggren et al.[93] in the dinuclear manganese complexes **10** $[Mn^{IV}Mn^{IV}(\mu\text{-}O)_2(L1)_2]^{2+}$ {HL1 = 2-[({2-[bis(pyridin-2-ylmethyl)]amino}ethyl)(methyl)amino]acetic acid} and **11** $[Mn^{III}Mn^{IV}(\mu\text{-}O)_2(L2)_2]^{+}$ {HL2 = *N*,*N*-bis(2-pyridylmethyl)glycine} (Figure 3). Both complexes showed similar cyclic voltammetry in acetonitrile with quasi-reversible reduction waves assigned to $Mn^{IV}Mn^{IV}/Mn^{III}Mn^{IV}$ and $Mn^{III}Mn^{IV}/Mn^{III}Mn^{III}$ redox couples, respectively.[94]

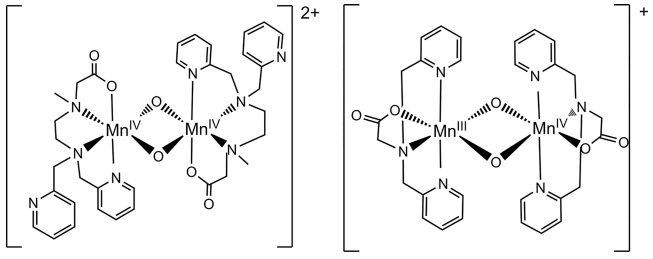

Figure 3. Complexes **10** and **11**.

Comparison of the FTIR spectra of complexes **10** and **11** in CD_3CN in different oxidation states showed that all of the carboxylato bands were affected by the reduction and/or the overall change in charge of the complexes, with the Δ value [$\Delta = \nu_a(COO) - \nu_s(COO)$] changing for the $Mn^{IV}Mn^{IV}$ to $Mn^{III}Mn^{IV}$ reduction by 70–125 cm^{-1} and to

a lesser extent (60–80 cm^{-1}) for the $Mn^{III}Mn^{IV}$ to Mn^{III}-Mn^{III} reduction. In contrast to that observed for monodentate carboxylates, for the complex $[Mn_2(\mu\text{-}O)(\mu\text{-}OAc)_2(tacn)_2]^{n+}$ (**12**, Figure 1), the Δ value increased upon reduction from the $Mn^{III}Mn^{IV}$ (n = 3) to the $Mn^{III}Mn^{III}$ state (n = 2) for the bridging μ-carboxylato ligands in the latter complexes.[95,96] The data indicated that significant changes in the IR active carboxylato stretching modes can be expected for monodentate carboxylato ligand upon a change in the oxidation state of the manganese ions.

As part of an effort to understand the effect of water on the redox properties of synthetic OEC mimics, Kurz et al.[97] studied the redox behaviour of the dinuclear complex $[Mn^{III}Mn^{III}L(\mu\text{-}OAc)_2]^+$ (**13**) (where L is the trianion of 2,6-bis{[(3,5-di-*tert*-butyl-2-hydroxybenzyl)(2-pyridylmethyl)amino]methyl}-4-methylphenol) (Figure 4). The presence of up to 0.5 M water in acetonitrile did not affect the coordination of acetato ligands to the complex significantly, based on ESI-MS data. Cyclic voltammetry of **13** showed that its oxidation occurred at less positive potentials in the presence of water, however.

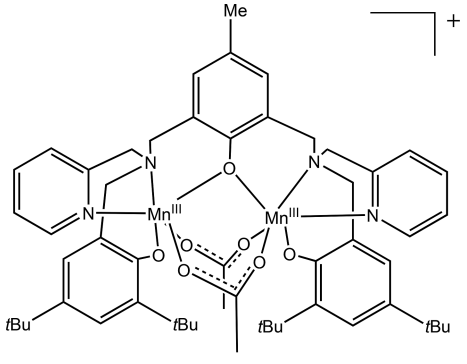

13

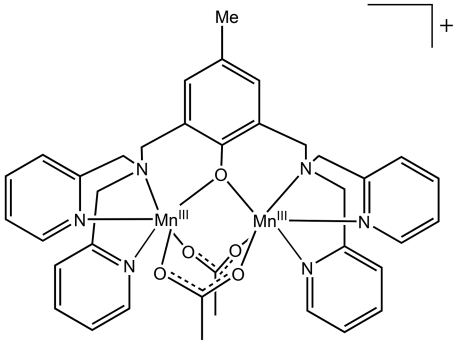

14

Figure 4. Structure of **13** and **14**.

With 5 M water, part of **13** re-reduced at 0.2 V, indicating the occurrence of a prior rapid equilibrium. Bulk electrolysis in the presence of water followed by UV/Vis absorption spectroscopy showed that one-electron reduction to the $Mn^{II}Mn^{III}$ state resulted in a hypochromic shift and decrease in absorbance; the appearance of a ca. 2000 G wide multiline signal centred at $g \approx 2$ with ca. 150 G line spacing was assigned to a $Mn^{II}Mn^{III}$ species. A further one-electron reduction resulted in only a broad absorption remaining at greater than 350 nm and a change to a 25-line signal at $g \approx 2$, ascribed to a $Mn^{II}Mn^{II}$ or to a $Mn^{II}Mn^{III}$ species that had undergone significant structural changes compared with the one-electron reduced species **13**.[98–100] The changes were reversed fully upon reoxidation to the $Mn^{III}Mn^{III}$ state.

As expected, **13** is EPR silent in acetonitrile at 5 K;[98] however, after oxidation in the presence of 0.5 M water, a 16-line spectrum centred at g = 2, typical for a $Mn^{III}Mn^{IV}$ species with a single (μ-oxido)-bridge, was observed. Comparison of the EPR spectrum of **13** in anhydrous acetonitrile with that of **13** with water present (at ca. 0.5 M) indicated that water stabilised the $Mn^{III}Mn^{IV}$ state. At higher concentrations of water (> 5 M), monomeric Mn^{II} species were observed, manifested by the presence of a 6-line signal superimposed on the 16-line signal. It was concluded that reduction of **13** in CH_3CN/H_2O did not result in a change in coordination mode, with only a fraction of the $Mn^{II}Mn^{II}$ species undergoing ligand rearrangement to yield the species responsible for the 25-line EPR signal. Oxidation of **13** led to formation of $Mn^{III}Mn^{IV}$ complexes, which, in the presence of water, underwent replacement of one or both of the acetato ligands to form μ-oxido bridge(s) between the manganese centres and thereby stabilise the higher oxidation states. These changes in coordination mode could also be induced by chemical oxidation and reduction.

Eilers et al.[101] have studied the structural rearrangements that the complex $[Mn^{II}Mn^{II}(bpmp)(\mu\text{-}OAc)_2]^+$ {**14**, bpmp = 2,6-bis[bis(2-pyridylmethyl)amino]methyl-4-methylphenol anion} undergoes in the presence of water. In anhydrous acetonitrile, **14** undergoes two quasi-reversible oxidations (Figure 5). Addition of water (10% v/v) resulted in a broadening of the second oxidation wave, together with a loss of reversibility and the appearance of an additional reduction wave at 0.2 V (vs. $Fc^{+/0}$) on the return cycle. The irreversibility was assigned to a charge compensating ligand-exchange reaction in which one of the μ-OAc was replaced by a μ-O bridge and the new reduction wave was assigned to the reduction of one of the products formed. The additional reduction wave was irreversible, which also indicated that the initial product converts into the original complex rapidly and quantitatively. It should be noted that the first oxidation wave was essentially unperturbed by addition of water, indicating that the $Mn^{II}Mn^{III}$ state is stable with regard to changes in ligand coordination.

From FTIR spectroscopic analysis, in CH_3CN with D_2O, it was apparent that the $Mn^{II}Mn^{II}$ and $Mn^{II}Mn^{III}$ complexes show less tendency to undergo exchange of the acetato ligands with water than does **14** in its $Mn^{III}Mn^{III}$ oxidation state. Furthermore, the absence of IR absorption from acetic acid indicated that water binds as aquo rather than in the hydroxido or oxido form.[102]

Anderlund et al.[103] reported a di-μ-acetato bridged dinuclear manganese complex, $\{[Mn^{II}Mn^{III}L(\mu\text{-}OAc)_2]^+\}$ (**15**), with a non-symmetric ligand, L = 2-{[bis(pyrid-2-ylmethyl)amino]methyl}-6-{[(3,5-di-*tert*-butyl-2-hydroxybenzyl)(pyrid-2- ylmethyl)amino]methyl}-4-methylphenol, that

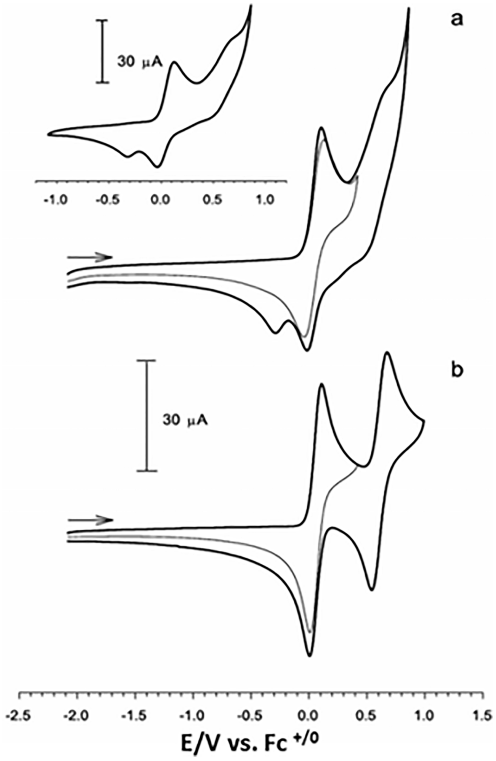

Figure 5. Cyclic voltammograms (0.100 V s^{-1}) of **14** (2 mM) in CH_3CN with (a) 10% (v/v) of water and (b) neat CH_3CN with 0.1 M [(n-C_4H_9)N][ClO_4] as supporting electrolyte. Inset: Second cycle. Reproduced with permission from ref.[101] Copyright RSC (2005).

provided N_3O_3 and N_2O_4 coordination at the Mn^{n+} and $Mn^{(n+1)+}$ centres, respectively (Figure 6).

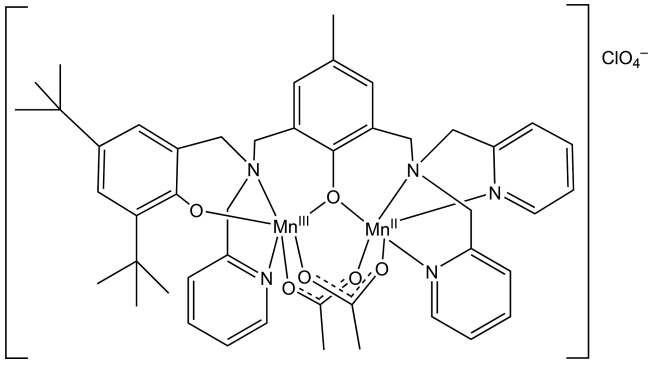

Figure 6. Complexes **15**.

The crystal structure of the complex showed that the terminal phenoxyl ligand coordinated to the Mn^{III} centre rather than to the Mn^{II} centre. The assignment of $Mn^{II}Mn^{III}$ redox state was confirmed by its magnetic moment of 7.20 BM at room temperature, which is slightly lower than the expected value of 7.6 BM, and at low temperature of 1.79 BM, which was close to the expected 1.73 BM. FTIR spectroscopy showed absorption bands at 1590 cm^{-1} (s, ν_aC–O, carboxylato); 1441 cm^{-1}(s, ν_sC–O, carboxylato) in the solid state and the similarity with the spectrum of the complex in anhydrous CD_3CN confirmed that the di-μ-acetato bridging remained intact upon dissolution.

One-electron reduction, by electrolysis at –0.93 V, resulted in the appearance of an EPR spectrum (at 12 K) that was typical of a weakly coupled [$Mn^{II}Mn^{II}$L(μ-$OAc)_2$] complex together with a loss of visible absorbance. The $Mn^{II}Mn^{III}$ complex was recovered after reoxidation at 0.08 V. Bulk electrolysis at 0.57 V yielded an EPR silent product, which was assigned to a $\{Mn^{III}Mn^{III}(\mu\text{-}OAc)_2\}^{2+}$ core. The product of the electrolysis at 0.82 V was not identified because of the instability of the oxidised complex, ascribed to oxidative degradation of the ligand and liberation of Mn^{II}, as observed by EPR spectroscopy.

The redox properties of **15** were compared to those of the symmetric analogues [$Mn^{II}Mn^{II}$(bpmp)(μ-$OAc)_2$]$^+$ (**14**) and [$Mn^{III}Mn^{III}$(bhpp)(μ-$OAc)_2$]$^+$ {**17**, where bhpp is 1,4-bis[(2-hydroxybenzaldehyde)propyl]piperazine}, which present $(N_3O_3)_2$ and $(N_2O_4)_2$ donor sets, respectively.[98,104] Higher oxidation states were found to be stabilised by the increase in the number of oxygen donors; however, metal oxidation states higher than $Mn^{III}Mn^{III}$ could not be obtained by bulk electrolysis in non-aqueous solvents.

The presence of bridging acetato ligands in all three oxidation states $Mn^{II}Mn^{II}$, $Mn^{II}Mn^{III}$ and $Mn^{III}Mn^{III}$ was confirmed by FTIR spectoelectrochemistry with $\Delta\nu = \nu_{as} - \nu_s$ for the acetato ligand of 120, 170 and 220 cm^{-1}, respectively.[101] Ligand exchange reactions for **15** and the oxidation states higher than $Mn^{II}Mn^{III}$ were also investigated in aqueous acetonitrile. An increase in water concentration resulted in depletion and replacement of the bands of the bridging acetato ligands (ν_{as}, 1590 cm^{-1}, ε = 4170 M^{-1} cm^{-1}) by the broader and weaker ν_{as} band of unbound acetate ions at lower frequency (1574 cm^{-1}, ε = 840 M^{-1} cm^{-1}). It was concluded that one of the acetate bridges was replaced readily by two terminal aqua ligands, whereas the second acetate remained coordinated even at the highest concentrations of water (up to 30 M) employed. In contrast, for the bpmp analogues, both of the acetato ligands were replaced under these conditions together with formation of both acetic acid and acetate. Oxidation of **15** in acetonitrile/water at 0.47 V (vs. $Fc^{+/0}$) to form the $Mn^{III}Mn^{III}$ complex and subsequent oxidation at 0.72 V vs. $Fc^{+/0}$ to generate the $Mn^{III}Mn^{IV}$ state led to the appearance of acetic acid (1725, 1380 and 1300 cm^{-1}), which confirmed that the water-derived ligands are at least partly deprotonated upon oxidation of the Mn centres. Hence, in higher oxidation states, the water-derived ligands are present as oxido- or hydroxido-bridges.

Complex **15** undergoes photooxidation to a $Mn^{III}Mn^{IV}$ complex in the presence of $[Ru^{II}(bpy)_3]^{3+}$ and the electron acceptor $[Co^{III}(NH_3)_5Cl]^{2+}$, in aqueous organic solution.[97] It was proposed that the product bears a di-μ-oxido or di-μ-oxido/hydroxido bridging motif in place of the μ-acetato ligands. Further photoinduced oxidation of this complex might result in the formation of a $Mn^{IV}Mn^{IV}$ or Mn^{III}-Mn^{IV}L* product with a ligand-based radical. The estimated redox potential of the $Mn^{III}Mn^{IV}/Mn^{III}Mn^{III}$ couple of the $Mn^{III}Mn^{IV}$ complex obtained was within a desirable poten-

tial range with respect to the average potential of 0.81 V vs. NHE (at pH 7) required for water oxidation.

The key attraction of multinuclear manganese complexes based on the 1,4,7-triazacyclononane (tacn) family of ligands is their thermodynamic stability and extensive redox and coordination chemistry. In the mid-1980s, complexes based on this ligand and its analogues were studied spectroscopically and electrochemically by Wieghardt et al.,[95,96] with a focus on mimicking the structure and function of manganese-based enzymes.[105] Application to laundry cleaning was reported in the mid-1990s.[106] Hage et al.[53] described the pH dependence of the physical and electronic properties of $[Mn^{IV}Mn^{IV}(\mu\text{-}O)_3(tmtacn)_2]^{2+}$ (**18**) in CH_3CN and water. Complex **18** undergoes protonation only with concentrated strong acids (e.g., H_2SO_4, $HClO_4$). The ν_{as} (670 cm^{-1}) and vs. (701 cm^{-1}, λ_{exc} = 488 nm) Mn–O–Mn vibrational modes in the IR and Raman spectra of **18**, respectively, were identified by ^{18}O-labelling. Protonation resulted in a shift in both bands to 683 cm^{-1} with an increase in the Mn–O–Mn angle (78° to 81°).[107] The reduction potential of **18** is surprisingly negative, given that the complex is in the $Mn^{IV}Mn^{IV}$ oxidation state and was attributed to the strong σ-donor properties of the three μ-oxido ligands.[108] The EPR spectrum of the $Mn^{III}Mn^{IV}$ species generated by using the one-electron reductant $Co(Cp)_2$ showed the characteristic 16-line spectrum with a hyperfine coupling constant (α_{Mn}) of ca. 69 G at 77 K.[109–111] In acetonitrile, it was proposed that the reduced species contained either a $Mn^{III}Mn^{IV}(\mu\text{-}O)_3$ core or a $Mn^{III}Mn^{IV}(\mu\text{-}O)_2(\mu\text{-}OH)$ core with similar Mn–O–Mn angles to those of the parent compound on the basis of FTIR and UV/Vis spectroelectrochemistry. The band at 668 cm^{-1} [$\nu_{as}(Mn\text{–}^{I6}O\text{–}Mn)$] reflects the Mn–O–Mn bond angle and does not change upon reduction. The bands at 791, 990 and 1007 cm^{-1} decreased in intensity and a new band at 1016 cm^{-1} appeared. Similarly, in aqueous solution, reduction of **18** also leads to a complex with a $Mn^{III}Mn^{IV}(\mu\text{-}O)_2(\mu\text{-}OH)$ core; however, in citrate buffer a positive shift in reduction potential is observed below pH 4, consistent with a $1e^-/1H^+$ coupled reduction. As would be expected, in the one-electron reduced state (i.e., $Mn^{III}Mn^{IV}$), the pK_a (protonation of one of the μ-oxido ligands) increased to ca. 4. Notably, however, reductive bulk electrolysis of **18** in aqueous citrate buffer at pH 3.5 resulted in the appearance of two absorption bands at 485 and 515 nm and a weak band at 725 nm, which are characteristic of a $[Mn^{III}Mn^{III}(\mu\text{-}O)(\mu\text{-}RCO_2)_2(tmtacn)_2]^{2+}$ species[96] rather than to **18** in the $Mn^{III}Mn^{IV}$ oxidation state.

Although Mn-tmtacn complexes were shown to be catalytically active in oxidations with H_2O_2 (see below), already in the mid-1990s,[106] it was discovered that certain additives[112–116] can play a role in enhancing their catalytic performance, which prompted renewed interest in the redox- and solvent-dependent coordination chemistry of the complexes. One such class of additives were carboxylic acids. As will be discussed below, the conversion of the tris-μ-oxido bridged complex **18** into bis-μ-carboxylato complexes such as **7**–**9** was found to be central to the catalytic activity observed in several cases.[117,118] This reaction re-

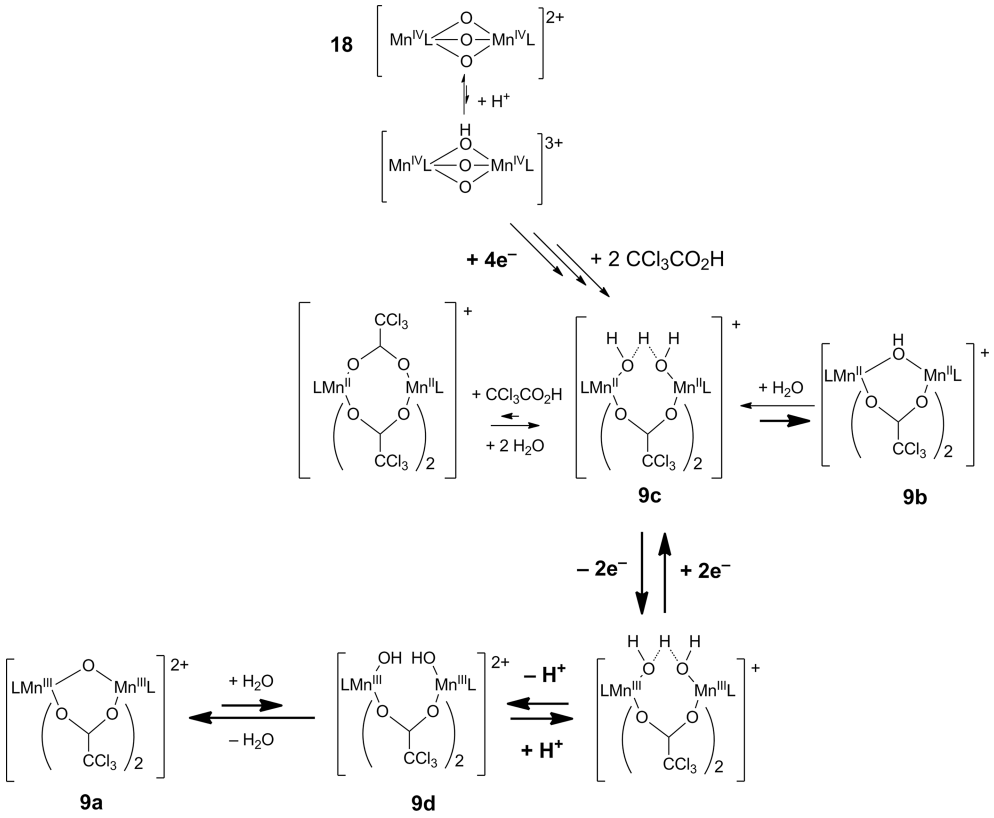

Scheme 2. Summary of redox chemistry of **18** and **9a**–**d** in 0.1 M $TBAPF_6/CH_3CN$ in the presence of CCl_3CO_2H (L = tmtacn).[92]

quires reduction of **18** from a $Mn^{IV}Mn^{IV}$ oxidation state to a $Mn^{III}Mn^{III}$ state, together with exchange of two μ-oxido ligands with two μ-carboxylato ligands. In an effort to understand this process in detail, de Boer et al.[92,119] investigated the redox-dependent coordination chemistry of both **18** and bis-μ-carboxylato species, such as **9a**, under conditions employed in the catalytic oxidation of alkenes. A relatively complex, but nevertheless well defined, interplay was noted between redox state, pH, carboxylic acid and water in determining both the initial conversion of **18** and the species present under catalytic conditions (Scheme 2).

As noted by Hage et al.,[53] the one-electron reduction of **18** at –600 mV (vs. SCE) undergoes a shift and becomes an irreversible four-electron reduction at ca. –0.2 V in the presence of carboxylic acids in water. de Boer et al.[92] observed a similar effect of carboxylic acid in acetonitrile. The species formed initially upon reduction is the colourless $Mn^{II}Mn^{II}$ complex **9c**, which can undergo subsequent oxidation to form initially the Mn^{III}_2 complexes **9d** followed by a loss of H_2O to form **9a** (Figure 7 and Figure 8). In contrast to trichloroacetic acid, when acetic acid is present, the μ-oxido bridged dinuclear complex **18** is formed immediately upon oxidation, which is consistent with ESI-MS data for the effect of the carboxylato ligand on ^{18}O exchange (see above).

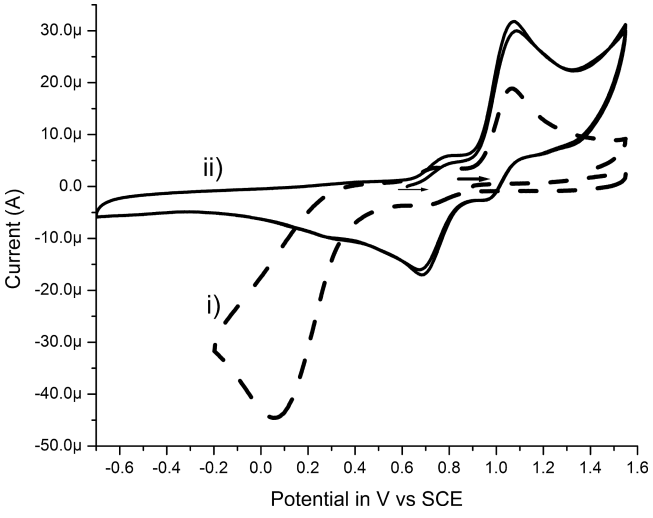

Figure 7. Cyclic voltammogram of **18** in CH_3CN (0.1 M KPF_6) (a) with 10 equiv. CCl_3CO_2H 0.1 $V s^{-1}$ in CH_3CN/0.1 M KPF_6, before (i) and after (ii) bulk reduction at –0.2 V. Reproduced with permission from ref.[92] Copyright ACS (2007).

The redox chemistry of **9a** highlights the interplay of redox state, H_2O and pH in controlling the coordination chemistry of manganese complexes. The μ-hydroxido bridged $Mn^{II}Mn^{II}$ complex **9b** undergoes reversible one-electron oxidation to $[Mn^{II}Mn^{III}(\mu\text{-OH})(\mu\text{-}CCl_3CO_2)_2(tmtacn)_2]^{2+}$ at 0.53 V in acetonitrile (Figure 9). Addition of carboxylic acid, however, results in the immediate opening of the μ-oxido bridge to form the $\{Mn^{II}Mn^{II}(\mu\text{-}O_2H_3)\}$ complex **9c**. In the presence of CCl_3CO_2H, **9c** undergoes a two-electron oxidation at $E_{p,a}$ = 1.03 V (vs. SCE) to a $\{Mn^{III}Mn^{III}(\mu\text{-}O_2H_3)\}$, which is more acidic and undergoes

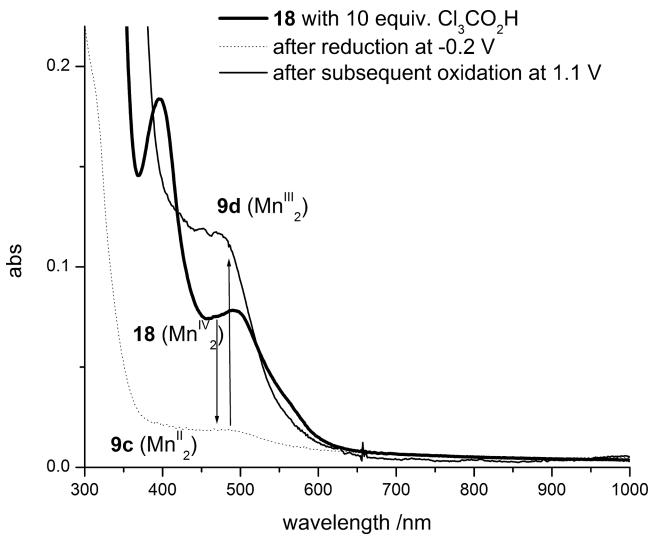

Figure 8. UV/Vis spectroscopy of **18** (1 mM) with CCl_3CO_2H (10 mM) in CH_3CN/0.1 M KPF_6. Before (thick line) and after (dotted line) bulk reduction at –0.2 V, and after bulk reoxidation at 1.1 V (thin line). Reproduced with permission from ref.[92] Copyright ACS (2007).

deprotonation to form the $\{Mn^{III}Mn^{III}(\mu\text{-OH})_2\}$ species **9d** (Scheme 2).

The $Mn^{III}Mn^{III}$ complex **9a**, which is the primary species observed under catalytic conditions, undergoes a reversible oxidation to the $Mn^{III}Mn^{IV}$ state and reversible one-electron reduction to the $Mn^{II}Mn^{III}$ oxidation state (Figure 8). Addition of 1 equiv. or more of a carboxylic acid resulted in the reduction changing to an irreversible two-electron process. Thin-layer voltammetry demonstrated that the product of the reduction was **9c**.

Overall it can be concluded that the rates of exchange of bridging oxido and carboxylato ligands, which are of particular relevance to biological systems, are heavily affected by both oxidation state and the electron-donating ability of the ligands. Lower oxidation states, in addition to higher exchange rates, also tend to favour the less strong sigma-donor carboxylato over oxido and hydroxido ligands. The mechanism of exchange appears to follow a general trend of protonation of the oxido bridging ligands followed by exchange with water or carboxylates. Understanding the intimate relationship between changes in redox state and changes in the coordination environment of multinuclear manganese complexes is essential for elucidating the mechanistic pathways through which such complexes engage.

2.4. Manganese-Catalysed Disproportionation of H_2O_2

Catalase enzymes protect cells from oxidative stress by disproportionation of H_2O_2 into O_2 and H_2O, through sequential oxidation and reduction of H_2O_2. Many catalase enzymes are based on iron, however, several enzymes utilise manganese including those isolated from *Lactobacillus plantarum*,[120] *Thermus thermophilus*[121] and *Thermoleophi-*

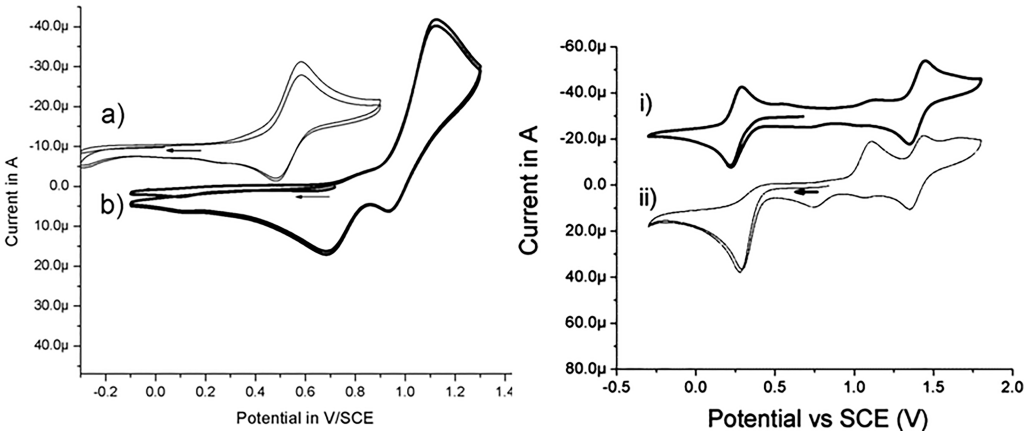

Figure 9. (left) Cyclic voltammetry of **9b** (1 mM) in CH_3CN/0.1 M (TBA)PF_6 in (a) the absence and (b) the presence of 10 mM CCl_3CO_2H. Initial scan direction from the open circuit potential is cathodic in each case. Scan rate: 0.1 $V s^{-1}$. (right) Cyclic voltammetry of **9a** (1 mM) in CH_3CN/0.1 M (TBA)PF_6 (i) in the absence and (ii) in the presence of 10 mM CCl_3CO_2H. Reproduced with permission from ref.[92] Copyright ACS (2007).

lum album.[122,123] Catalases containing a binuclear manganese active site have been proposed to employ a {Mn(μ-RCO_2)(μ-O/OH)Mn} structural unit with coordination by histidine and glutamate side chains and a range of Mn^{II}-Mn^{II}, $Mn^{II}Mn^{III}$, $Mn^{III}Mn^{III}$ and $Mn^{III}Mn^{IV}$ oxidation states.[19,124] H_2O_2 disproportionation is achieved by such catalases through cyclical changes in the bridging ligands that accompany the changes in redox state; that is, in *T. thermophiles* catalase, a μ-carboxylate ligand (Glu), a μ-OH, and a μ-OH_2 are present in the $Mn^{II}Mn^{II}$ oxidation state, whereas a μ-oxido bridge is present in the $Mn^{III}Mn^{III}$ oxidation state.[125] The design of manganese complexes that engage in catalase activity has received considerable attention over the last decades, focusing on the effect of redox state, redox potential, nuclearity, coordination asymmetry and inner-sphere ligand rearrangements.[110,126,127,128] However, elucidating the mechanisms by which catalysts disproportionate H_2O_2 is highly challenging because of the high turnover frequencies encountered; hence, typically only the resting state of the catalyst is observable.

A series of six-coordinate $Mn^{II}Mn^{II}$ and $Mn^{III}Mn^{III}$ complexes with binucleating salen type ligands and alkoxide bridges were reported as functional models for catalases,[110,129,130,131] albeit with catalytic efficiencies approximately 575 and 3160 times lower than those of *L. plantarum*[132,133] and *T. thermophiles* enzymes,[134] respectively. $[Mn^{IV}salpn(\mu\text{-}O)]_2$ {salpn = 1,3-bis(salicylideneamino)propane} is one of the more efficient functional mimics, however, in contrast to enzymatic systems, it cycles between $Mn^{IV}Mn^{IV}$ and $Mn^{III}Mn^{III}$ oxidation states.[135,136] Indeed, only a few of the reported synthetic catalase mimics operate through a $Mn^{II}Mn^{II}/Mn^{III}Mn^{III}$ redox cycle.[110,126,130,131,134,137,138] It was also demonstrated by reactions with deuterium peroxide that proton transfer plays an important role both in complex formation and in the rate-limiting step.[139]

Dismukes et al.[140] studied the effect of the bridging μ-hydroxide on μ-carboxylato coordination of manganese complexes in detail as a functional model of dimanganese catalases. Two $Mn^{II}Mn^{II}$ complexes and their corresponding $Mn^{III}Mn^{III}$ complexes, based on ligands containing N-alkylated benzimidazoles (Figure 10), were studied in solution in the presence of O_2 under basic conditions to elucidate the mechanism by which they disproportionate H_2O_2. Given that the structural changes that these complexes undergo are highly typical of dinuclear manganese complexes and give valuable insight into the driving force behind catalase activity, in the following section their chemistry will be discussed in more detail. Furthermore, this series of reports highlight the benefits of a multi-technique approach (i.e., UV/Vis absorption, EPR, ^1H NMR and FTIR spectroscopy and mass spectrometry) in speciation analysis.

The complexes **19**–**22** remain in the $Mn^{II}Mn^{II}$ oxidation state under anaerobic conditions, in methanol and acetone, but nevertheless undergo reversible pH dependent changes in the coordination of the alkyoxy bridge, hydroxido and carboxylato ligands. The EPR spectrum of **19** in acetone is similar to that of manganese catalase from *T. thermophiles* in its $Mn^{II}Mn^{II}$ oxidation state.[138c] In the presence of 5 vol.-% water, however, a characteristic six-line signal of a mononuclear Mn^{II} species at $g = 2$ and a broad low-field signal at 1100–1600 G were observed for **19**, attributed to a spin-uncoupled dinuclear $Mn^{II}Mn^{II}$ species. The six-line signal disappeared upon the addition of NaOH, whereas the intensity of the signals of the spin-coupled species increased. The addition of NaOD to a solution of **27** in MeOD resulted in a decrease in the ^1H NMR signal at δ = 22.8 ppm assigned to the methyl group of the bridging acetate[141] and to the appearance of a new signal at δ = 1.90 ppm, consistent with the conversion of the μ-bridging acetato ligand into a labile monodentate coordination mode. This monodentate ligand is in equilibrium with the unbound acetate, which appeared at δ = 1.89 ppm, hence the signal at δ = 1.90 ppm showed a large coupling constant (J = 24 Hz). The conversion of **21** from the $Mn^{II}Mn^{II}$ into the $Mn^{III}Mn^{III}$ oxidation state in methanol is reversed upon addition of DCl. The same behaviour was observed with **22**, in which a $\mu_{1,3}$-chloroacetato bridging ligand is present

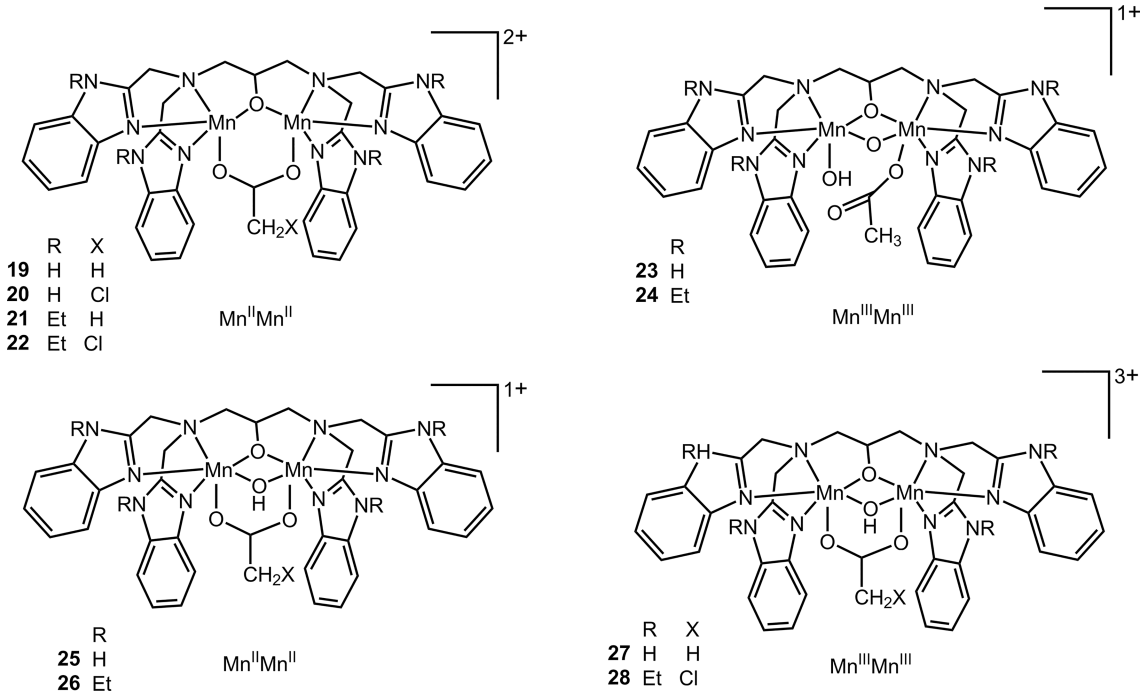

Figure 10. Structure of manganese complexes **19**–**28**.

instead of a μ-acetato bridge. In the case of **19** only six broad signals were observed by ^{1}H NMR spectroscopy upon addition of NaOD, which are assigned to the D_2O exchangeable protons on the benzimidazole moieties.

The coordination mode of the carboxylato group of the complexes was determined by FTIR spectroscopic analysis.[142] Complex **19** showed two modes at 1564 and 1427 cm^{-1} assigned to the asymmetric and symmetric stretching mode of a symmetrical μ-bridging acetato ligand ($\Delta\nu$ = 137 cm^{-1}). The FTIR spectrum of the $Mn^{III}Mn^{III}$ form of **19** showed absorptions at 1564 cm^{-1} that disappeared while a new strong absorption at 1627 cm^{-1} appeared, which was assigned to the monodentate coordinated acetate (the absorption from noncoordinated carboxylate appears at 1578 cm^{-1}). Furthermore, a new absorption band appeared between 583–590 cm^{-1} that was assigned to a (Mn–O–Mn) stretch.

The reversible protonation of the alkoxide moiety of the ligand, and its dissociation from one of the Mn^{II} centres, in the presence of water was proposed based on these data.

The UV/Vis absorption spectra in methanol of complexes **19**–**22**, in the $Mn^{II}Mn^{II}$ oxidation state, are unaffected by addition of hydroxide in the absence of oxygen. In the presence of oxygen however, three absorption bands appeared at 425, 472 and 760 nm, which were assigned to ligand field transitions of Mn^{III} or $Mn^{III}Mn^{III}$ complexes in low symmetry environments (or possibly LMCT transitions) based on earlier studies of the reaction between **19** and H_2O_2. The observation that **21**, which is based on N-alkylated benzamidazoyls, shows the same changes as those of **19** and **20** confirms that the changes are not due to simple deprotonation of the benzimidazole groups. Furthermore, under basic conditions in the presence of oxygen, the EPR signals related to the $Mn^{II}Mn^{II}$ species diminished, which is consistent with the formation of dinuclear $Mn^{III}Mn^{III}$ species. These data indicate the ease with which the $Mn^{II}Mn^{II}$ complex can undergo oxidation when stabilised by anionic ligands.

Although signals were not observed for **19** or **20** by ESI-MS, signals were observed for **21** and **22** with a base signal at *m/z* 989 for **21** assigned to $\{[L^2Mn^{II}Mn^{II}(\mu\text{-OAc})](ClO_4)\}^+$. Its intensity decreased upon addition of NaOH and two new signals appeared at *m/z* 1048 and 949 assigned to $\{[L^2Mn^{III}Mn^{III}(\mu\text{-O})](ClO_4)_2\}^+$ and $\{[L^2Mn^{III}Mn^{III}(\mu\text{-O})](ClO_4)\}^{2+}$. Notably, no evidence for an acetato ligand bound to the $Mn^{III}Mn^{III}(\mu\text{-O})$ complex was obtained in the presence of more than 2 equiv. of NaOH, whereas for the $Mn^{II}Mn^{II}$ complexes of **19** and **21**, a bound acetate was observed (Scheme 3). It was suggested that there is an unbound or weakly bound acetate that dissociated under the conditions of the ESI-MS for the oxidised complex $Mn^{III}Mn^{III}$, because a bound monodentate acetate was observed by ^{1}H NMR spectroscopic analysis (see above).

In summary, carboxylato and hydroxido ligands undergo relatively facile exchange when the complex is in the $Mn^{II}Mn^{II}$ oxidation state, with both monodentate and bridging coordination modes being observed for both ligands (Scheme 4). These changes in coordination mode of the carboxylato ligand, from bidentate to monodentate, are central to allowing other small molecules to bind to the manganese ions, in a process referred to as a carboxylate shift, to provide a free site on the manganese centre for coordination. Importantly, as the oxidation state is increased, the exchange of carboxylato ligands for oxido ligands and especially bridging oxido ligands becomes in-

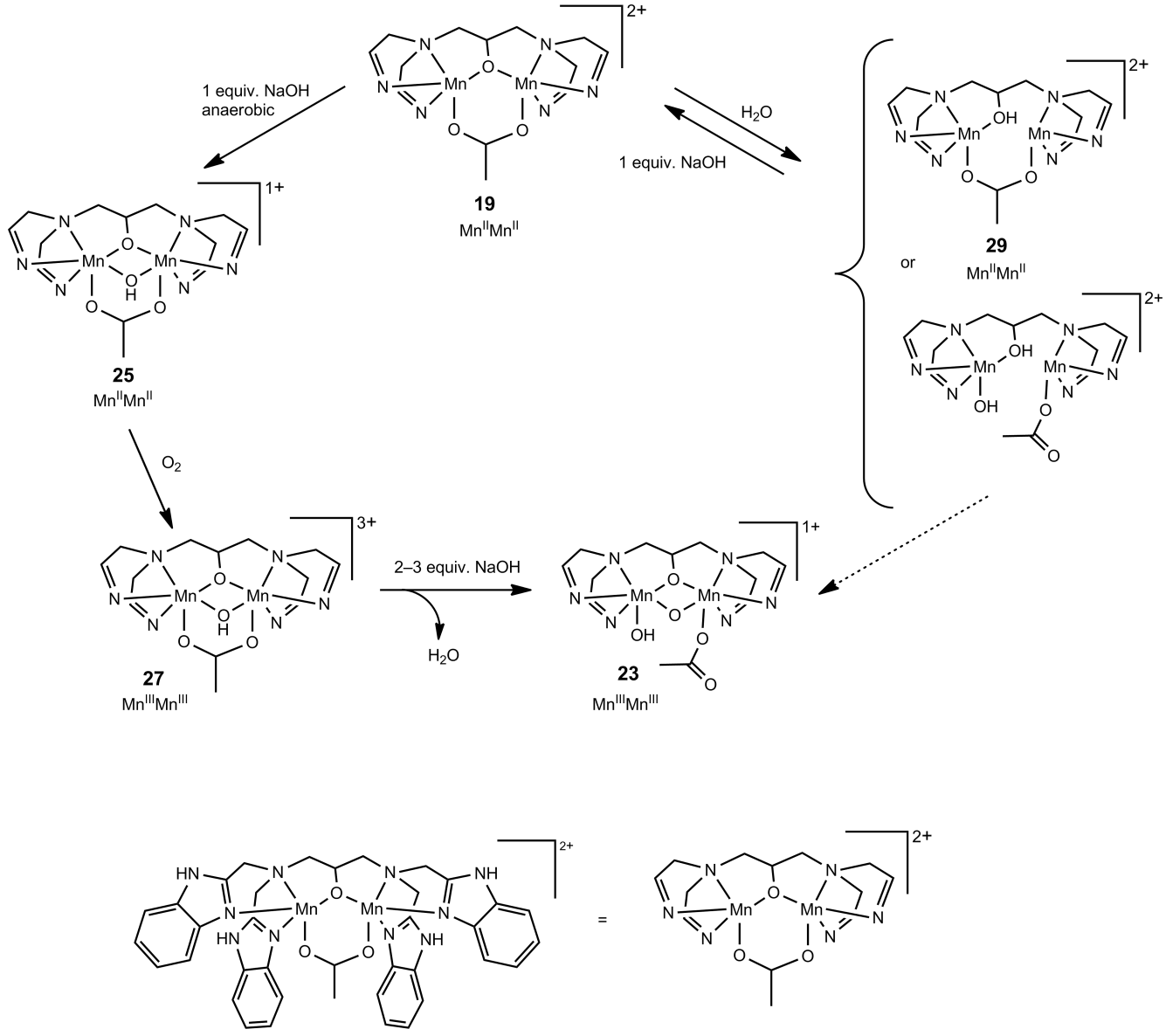

Scheme 3. Structural changes occurring upon addition of NaOH to **19** in acetone.

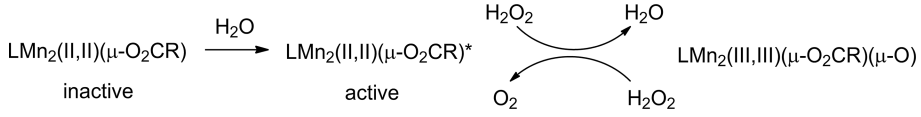

Scheme 4. Activation and catalytic cycling between $Mn^{II}Mn^{II}$ and $Mn^{III}Mn^{III}$ redox states.

creasingly pronounced, and is driven, in part, by the stabilisation that these more electron-rich ligands provide.

The redox state and hydroxide dependence of the coordination chemistry of **19** provided a basis for understanding the detailed mechanism involved in the disproportionation of H_2O_2 catalysed by these complexes.[137] The decomposition of H_2O_2 in methanol by **19** is characterised by a lag phase, which is decreased by pre-equilibration of the complex with ca. 2 vol.-% water. In addition, the reaction rate was increased 5–6 fold by addition of water. A Michaelis–Menton model for the reaction, i.e., binding of peroxide to the catalyst followed by release of water and oxygen, was assumed, and the k_{cat} and K_m values for **19** showed a catalytic efficiency (k_{cat}/K_M) 10^5–10^6 times lower than those of catalase enzymes from *T. thermophilus*[134] and from *T. album*.[132] Further reductions in lag time or increase in reaction rate were not observed upon further increases in the water content. The effect of water was proposed to be due to dissociation of the μ-acetato ligand and, indeed, addition of excess acetate resulted in an increase in the lag phase and reduction in reaction rate. Notably, addition of 1 equiv. of NaOH removed the lag phase completely and resulted in

an increase in reaction rate with the observed rate constant (k_{obs}) of 1 $M^{-1}s^{-1}$ increasing to 92 $M^{-1}s^{-1}$ (with 5 equiv. of NaOH) and to 100 $M^{-1}s^{-1}$ (with 8 equiv. of NaOH). The increase in reaction rate was ascribed to the deprotonation of the H_2O_2. Similar behaviour was observed with **21**, indicating again that deprotonation of the benzimidazoles in **19** was not involved, and is consistent with the formation of the complex $[LMn^{II}Mn^{II}(\mu\text{-}OH)(\mu\text{-}OAc)]^+$.[140] It was proposed that, upon the addition of water, $[LMn^{II}Mn^{II}(\mu\text{-}OH)(\mu\text{-}OAc)]^{2+}$ is formed, which deprotonates spontaneously to form the catalytically active species $[LMn^{II}Mn^{II}(\mu\text{-}OH)(\mu\text{-}OAc)]^+$ (**25**) and the (inactive) $[LHMn^{II}Mn^{II}(\mu\text{-}OAc)]^{3+}$ (**29**), which was observed by EPR spectroscopy as a spin-uncoupled Mn^{II} species and shows lower activity towards H_2O_2 disproportionation. Hence, only a partial elimination of the lag phase was observed in the presence of water. In contrast to the decrease in the reaction rate upon the addition of more than 2% water without hydroxide, increasing the amount of water from 98:2 v/v methanol/water to 11:89 v/v methanol/water for **29** and the presence of 5 equiv. NaOH resulted in an increase in the k_{obs} from 9.2 to 24.8 $M^{-1}s^{-1}$, which was attributed to an enhancement of the rate of proton exchange. In the presence of the noncoordinating base 2,6-di(tertbutyl)pyridine, no change in the lag phase nor in O_2 evolution rate was observed for complexes **19**–**22**, confirming that ligand deprotonation is not involved.

The ^1H NMR spectrum of **23** (which was generated by addition of 4–5 equiv. of NaOH to **21**) in CD_3OD was similar to that of **27** (which was obtained by addition of 1 equiv. of NaOH to **21**) after addition of 10 or 20 equiv. H_2O_2. The dependence of reaction rate on the concentration of **23** indicated that it is the resting state in the catalytic cycle. ^1H NMR spectra obtained under catalytic conditions showed only one $Mn^{III}Mn^{III}$ complex with two pairs of nonequivalent N–H protons and a monodentate acetato ligand on one of the manganese ions. It was also suggested that **27** and **23** are in equilibrium in aqueous solvents, and that the substitution of the hydroxido ligand by H_2O_2 is facilitated by protonation. The rate-limiting step in the H_2O_2 disproportionation was proposed to be the oxidation of the $Mn^{II}Mn^{II}$ to a $Mn^{III}Mn^{III}$ species. Hence, for **25**, which is oxidised at lower potentials than **19**–**22**, the 6.5-fold increase in k_{cat} was rationalised as being due to a lowering of the activation energy in the oxidation step.

Based on kinetic studies of the catalysed decomposition of H_2O_2 and also on previous speciation analysis of these complexes, the mechanism shown in Scheme 5 was proposed for the disproportionation of H_2O_2 catalysed by the hydroxide-containing derivatives of complexes **21** and **22**.

Complex **25**, which bears three μ-bridging anions, is in equilibrium with species **25a**, which bears a terminal acetate and aqua ligand. The increase in the rate of the reaction with complex **25** and **28a′** was proposed to be due to the lower activation barrier to oxidation compared with that of **19**, which does not bear an OH group. This hypothesis requires that the rate-limiting step is oxidation of **25** or **25a** to a $Mn^{III}Mn^{III}$ species such as **23**. The thermodynamically favourable displacement of H_2O by H_2O_2 (**25a** to **25b** to

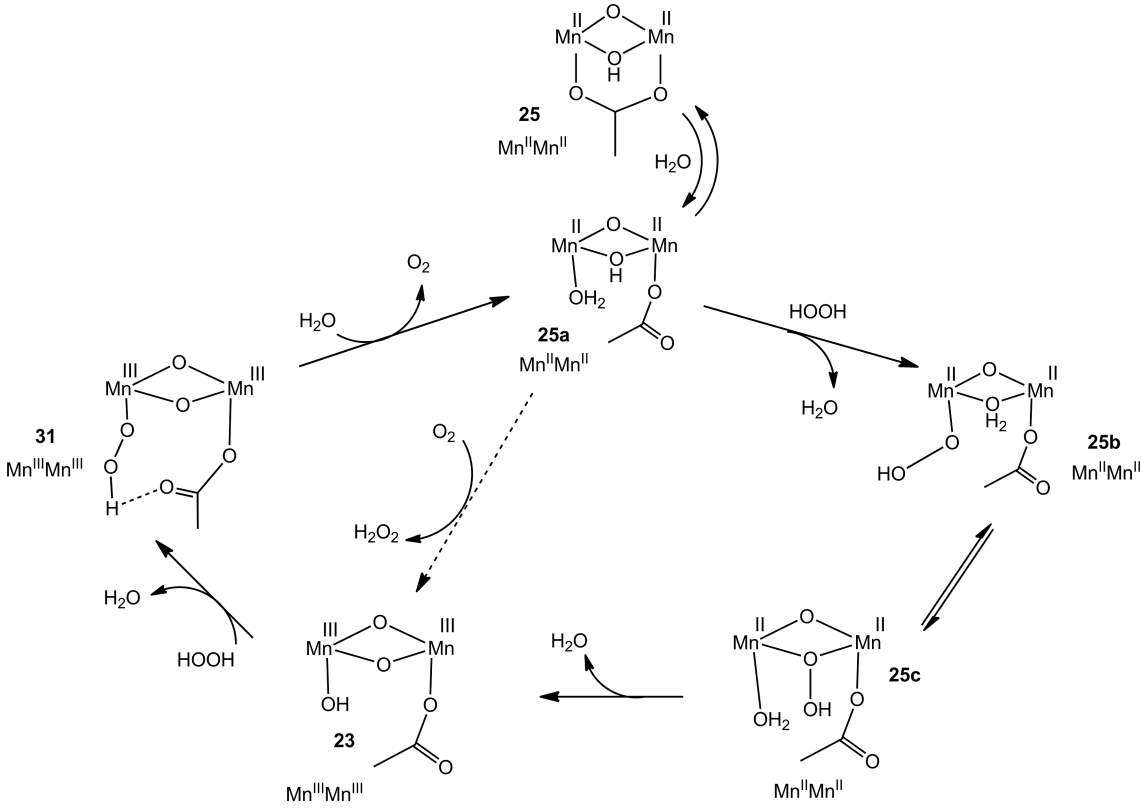

Scheme 5. Catalytic cycle for disproportionation of H_2O_2 by **19**–**22**.

25c) is facilitated by the presence of the hydroxide bridge,[140] and the propensity for the acetato ligand to switch between bridging and monodentate coordination. In the next steps (**25c** and **23**), cleavage of the μ-hydroperoxide ligand is coupled with oxidation of the $Mn^{II}Mn^{II}$ complex to the $Mn^{III}Mn^{III}$ state. Binding of a second molecule of H_2O_2 occurs and transforms **23** into **31** with stabilisation of **31** through intramolecular H-bonding between the terminal hydroperoxide and acetato ligand. The last step involves the re-formation of complex **25/25a** by protonation and reduction of **31** and formation of O_2.

The effect of base (specifically hydroxide) on the coordination chemistry of manganese complexes, and, in particular, the reversible displacement of carboxylato ligands is a general phenomenon and, as will be shown in the following selected examples, is a key driving force in cycle redox reactions in manganese catalysts.

Singorella et al.[143] reported a water-soluble $Mn^{III}Mn^{III}$ mimic of the active site of manganese catalases: Na-[$Mn^{III}Mn^{III}$(3-Me-5-SO_3-salpentO)(μ-OAc)(μ-OMe)(H_2O)]·4H_2O (**32**), for which 3-Me-5-SO_3-salpentOH = 1,5-bis(3-methyl-5-sulfonatosalicylideneamino)pentan-3-ol, and described its catalase activity in protic and aprotic solvents. The IR spectrum of **32** showed absorptions at 1558 and 1432 cm^{-1}, characteristic for the asymmetric and symmetric stretching vibrations of a μ-OAc ligand. The paramagnetic ^1H NMR spectrum of **32** in CD_3OD confirmed that this complex retained its dinuclear structure in solution. Addition of NaOH (from 1 to 5 equiv.) did not result in a change in the aromatic hydrogen signals, but the intensity of the hydrogen signals of the bridging acetato decreased and eventually disappeared upon addition of 5 equiv. base. These observations, together with ESI-MS, suggested that, in basic solution, the bridging acetato is converted into a monodentate terminal ligand.

The exchange of the carboxylato ligand with hydroxide and hydroperoxide[144] in five complexes [$Mn^{III}Mn^{III}$(μ-4-$RC_6H_4COO)_2$(μ-O)(bpy)$_2$($H_2O)_2$]($NO_3)_2$ {R = Me (**33**), F (**34**), CF_3 (**35**), MeO (**36**) and *t*Bu (**37**)} was investigated by Corbella et al. Complexes **33**–**37** showed activity towards the catalytic disproportionation of H_2O_2 in CH_3CN at 25 °C, with the rate increasing with concentration. The efficiency of the complexes was found to correlate with Hammett parameters for the R groups of the carboxylato ligands: **36** (MeO) > **37** (*t*Bu) > **33** (Me) > **34** (F) > **35** (CF_3). The minor difference in the catalytic activity of **34** (F) and **35** (CF_3) was attributed to the difference in the structure of these complexes. UV/Vis absorption and EPR spectroscopy before and after addition of H_2O_2 indicated that $Mn^{II}Mn^{II}$ complexes were formed upon addition of H_2O_2, with no evidence for mixed-valence species such as $Mn^{II}Mn^{III}$ or $Mn^{III}Mn^{IV}$. The integrity of the complexes towards ligand dissociation was supported by their activity over multiple cycles of addition of H_2O_2 compared with that of $Mn^{II}(NO_3)_2$.

Latour and co-workers[145] studied the reactivity of complexes **38**–**41** to explore the influence of the number of carboxylato moieties in the tripodal ligands on electronic properties and activity towards H_2O_2 disproportionation, mimicking the carboxylato-rich active site of the manganese catalase enzymes (see above) (Figure 11). The corresponding $Mn^{III}Mn^{III}$(μ-O)$_2$ complexes were generated by one-electron reduction. ^{18}O labelling allowed for assignment of the Mn–O_{oxido} stretching band at 660 cm^{-1}. The results showed a trend in the exchange interaction, which became less antiferromagnetic in the order: **38** ($-J = 161 \pm 5$ cm^{-1}) < **39** ($-J = 142 \pm 5$ cm^{-1}) < **40** ($-J = 133 \pm 9$ cm^{-1}). This order corresponds with the strengths of the Mn–O_{oxido} bonds, as revealed by the structural and infrared studies, indicating that the nature of the carboxylato ligands affect the strength of the Mn–O–Mn bonds.

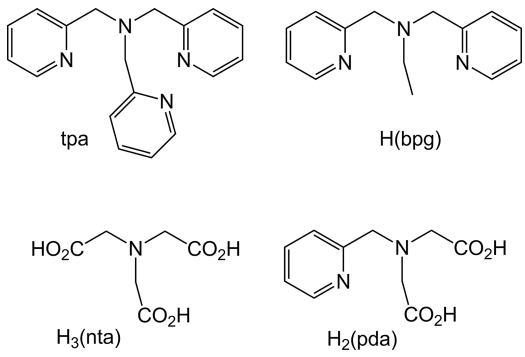

Figure 11. Structure of ligands used in the complexes **38**–**41**; [$Mn^{III}Mn^{IV}$(μ-O)$_2$(tpa)$_2$]($ClO_4)_3$ (**38**), [$Mn^{III}Mn^{IV}$(μ-O)$_2$(bpg)$_2$](ClO_4) (**39**), {[Mn_2(pda)$_2$(O)$_2$]Na($H_2O)_6$}$_n$ (**40**) and [Mn_2(O)$_2$(nta)$_2$]Na_3 (**41**) {where tpa = tris-picolylamine, H(bpg) = bis-picolylglycylamine, H_3(nta) = nitrilotriacetic acid, H_2(pda) = picolyldiglycylamine}.

Complex **38** and **39** showed two reversible redox couples [i.e., reduction to the $Mn^{III}Mn^{III}$(μ-O)$_2$ species and oxidation to the $Mn^{IV}Mn^{IV}$(μ-O) species]. Replacement of pyridine moieties by carboxylates lowered the oxidation potential of the $Mn^{III}Mn^{III}$/$Mn^{III}Mn^{IV}$ and $Mn^{III}Mn^{IV}$/$Mn^{IV}Mn^{IV}$ redox couples as expected due to stabilisation of higher oxidation states by anionic carboxylato ligands. The exchange of the μ-oxido ligands was determined in acetonitrile and acetonitrile/methanol (4:1) by ESI-MS and showed that replacement of pyridine moieties by carboxylates accelerated the rate of exchange. A similar effect was observed upon reduction of the {MnMn(μ-O)$_2$} core from the mixed-valent state {$Mn^{III}Mn^{IV}$} to {$Mn^{III}Mn^{III}$}, for which the exchange rate of μ-oxido ligands was increased by a factor of 84. Given that μ-oxido exchange involves the deprotonation of a molecule of water, it was suggested that the basic character of the carboxylate moiety could play a significant role in the observed rate enhancement.

Addition of $HClO_4$ to **38** in acetonitrile inhibited the disproportionation of H_2O_2, whereas addition of trimethylamine increased the reaction rate. These observations are consistent with the increase in H_2O_2 decomposition rate observed upon substitution of pyridine moieties by carboxylato moieties. In the case of the $Mn^{III}Mn^{IV}$ complexes, EPR spectroscopy showed that the 16-line spectrum was lost at the end of the reaction and was replaced by a poorly re-

solved six-line EPR spectrum typical of Mn^{II}. ESI-MS, together with $H_2{}^{18}O_2$ (3% in $H_2{}^{16}O$), showed that immediately after addition of H_2O_2, **39** incorporates oxido ligands from H_2O_2, which are lost subsequently by exchange with the $H_2{}^{16}O$; this suggested that the μ-oxido bridged complex is formed and broken in the catalytic cycle. The higher reaction rates observed for the carboxylate-bearing complexes was related to the ability of carboxylate ligands to act as internal bases. This effect is important in the catalase reaction because deprotonation of H_2O_2 provides protons for transfer to μ-oxido ligands, which can dissociate as water.

Overall, it can be concluded that in the functional models for dinuclear manganese based catalases, carboxylato shifts as well as exchange of bridging aqua ligands, is key to understanding the observed activity. Importantly, the changes in coordination mode as the redox state shuttles between lower and higher oxidation states make reduction and then oxidation of H_2O_2 thermodynamically feasible.

4. Mechanistic Studies in Manganese-Catalysed Alkene Oxidation in Organic Solvents

Catalytic activation of H_2O_2 and O_2 has been a highly active area of research over the last few decades, with catalysts based on transition metals at the forefront of these efforts; in particular those based on titanium,[146] vanadium,[147] rhenium[148] and tungsten,[149] primarily in their oxide forms and on iron, copper and cobalt, with carboxylate, amine and pyridyl based ligands. Manganese, the focus of the present review, and its complexes have seen widespread application in both fine and bulk chemical processes as catalysts for the activation of H_2O_2 especially.[3,7a] In the many oxidation reactions catalysed by manganese complexes, the active species involved in oxygen transfer and in C–H oxidation is frequently proposed to be a Mn^V=O moiety (e.g., LMn^V=O).[37,38,150,151] Observing such active species is, however, highly challenging and those Mn^V=O complexes that have been isolated from solution have been found to be either incapable of converting olefins into epoxides or relatively unreactive at most.[152–154] Isotope labelling with ^{18}O has therefore proven to be invaluable in establishing Mn^V=O species as active intermediates in olefin epoxidation.[32,155,156]

Manganese porphyrins and salen complexes have been studied intensively in epoxidations with a wide range of oxidants, primarily iodosylarenes, alkylhydroperoxides, *meta*-chloroperbenzoic acid (*m*CPBA) and hypochlorite.[7a] Activation of H_2O_2 is the primary focus of this review and a few examples of porphyrin complexes, employing H_2O_2 as terminal oxidant, have also been reported.[157] H_2O_2 disproportionation by manganese salen complexes usually competes with epoxidation, reducing the efficiency of the oxidant. However, additives with bulky groups, such as imidazoles and carboxylates, which promote the formation of the Mn^V=O intermediates, as ascertained by ESI-MS as the actual epoxidising species, improved the performance of these catalytic systems. For a detailed discussion of manganese porphyrin, Schiff base and salen[158] based systems, the reader is referred to several reviews covering these catalyst systems.[4] In this section, several examples of manganese-based catalytic systems will be discussed in regard to mechanistic insights gained.

Busch and co-workers have studied the complex $[Mn^{II}(Me_2EBC)](Cl)_2$, based on the cross-bridged cyclam ligand Me_2EBC (4,11-dimethyl-1,4,8,11-tetraazabicyclo[6.6.2]hexadecane), as a catalyst for oxidation reactions.[159] UV/Vis absorption spectroscopy of Mn^{II}, Mn^{III} and Mn^{IV} complexes of this ligand upon reaction with H_2O_2 or *t*BuOOH, in an aqueous solution, showed no evidence for the formation of a Mn^V–oxido species but, rather, $[Mn^{IV}(Me_2EBC)(OH)_2]^2$ was confirmed to be the dominant species under neutral and acidic conditions. The absence of a stable Mn^V species is understandable considering that the ligand lacks the stabilising π-systems present in porphyrins and salen-based ligands. It was proposed[160] that the dominant mechanism for epoxidation by Mn–Me_2EBC employing H_2O_2 is a Lewis acid activation pathway rather than a high-valent Mn-oxo pathway; that is, formation of $[Mn^{IV}(Me_2EBC)(O)(OOH)]^+$ from $[Mn^{IV}(Me_2EBC)\text{-}(O)\text{-}(OH)]^+$. This peroxy complex is an inorganic peracid and transfers an oxygen atom directly to alkenes in a manner similar to that observed with organic peracids (Scheme 6). This mechanism was supported by ESI-MS under catalytic conditions by the detection of a signal assignable to $[Mn^{IV}(Me_2EBC)(O)(OOH)]^+$. Subsequent DFT studies by Haras and Ziegler, also support a mode of action of these complexes that involves a Mn^{IV}–OOH species.[161]

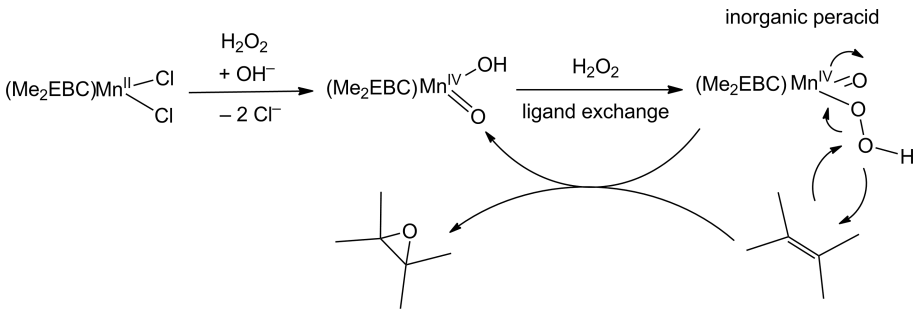

Scheme 6. Proposed Lewis acid activation mechanism for epoxidation of alkenes using $Mn^{II}(Me_2EBC)Cl_2$ and H_2O_2.[159]

4.1. Manganese-Catalysed Oxidations Involving in situ Generation of Catalysts from Well-Defined Manganese Complexes

In manganese-based catalyst systems, especially for alkene oxidation, the use of additives to suppress H_2O_2 disproportionation and to enhance catalytic activity has been widespread. Although this approach has increased dramatically the scope and activity of the catalysts, it has also raised many questions regarding the mechanism and the often complex roles the additives actually play. Furthermore, the initial form of the complex used as catalyst is not necessarily retained during catalysis and, indeed, different additives can lead to fundamentally different reaction pathways being followed by one catalyst, as will be highlighted in the following examples.

4.1.1. Manganese Polypyridyl Based Oxidation Catalysts

A rather extreme example of the changes that a catalyst undergoes to form the active catalytic species is found in a class of manganese complexes based on polypyridyl based ligands.[162] In early studies with this class of complexes it was concluded that high-valent manganese-oxido species were involved; however, as discussed above, such ligands are unlikely to stabilise such species. A key challenge presented by these systems with regard to mechanistic studies lay in the extensive disproportionation of H_2O_2 that competed with oxidation of substrates. The instability of this ligand class was first raised as an issue by Groni et al.[163] in the identification of products arising from oxidation at the benzylic positions of these ligands. Que[164] and, more recently, Britovsek[165] and co-workers have also noted these pathways for iron complexes.

Isolation of ligand degradation products by Pijper et al.[166] led to the realisation that under certain conditions, i.e., conditions used in several of the earlier studies[162] dealing with the oxidation of alkenes and alcohols, oxidative ligand degradation to pyridine-2-carboxylic acid (PCA) was occurring rapidly under the reaction conditions. Importantly, Pijper et al. demonstrated that it was, in fact, the thus formed PCA that was the ligand responsible for the epoxidation activity observed and not the polypyridyl ligands used initially (Scheme 7).

The manganese pyridine-2-carboxylic acid system subsequently developed by Saisaha[167] and Dong et al.[168] for the *cis*-dihydroxylation and epoxidation of alkenes, as well as alcohol and alkane oxidation,[169] presented a considerable challenge with regard to mechanistic studies because of the turnover frequencies (30 s^{-1}) and turnover numbers (> 300,000) that could be achieved and the low catalyst concentrations employed (as low as 10 μM), which essentially precludes direct spectroscopic detection of reactive intermediates. This challenge, however, does not mean that insight into the mechanism by which oxidation takes place cannot be gained by using spectroscopy. A key feature of the system is the formation of the catalyst in situ from PCA, a manganese salt, a base (e.g., NaOH or NaOAc) and, most importantly, a ketone.[168] The role of the ketone in the reaction was shown, by UV/Vis absorption and Raman spectroscopy, to be to form a hydroperoxide adduct. The hydroperoxide formed was found to be the active oxidant in the reaction and its formation was found to be rate controlling. The characteristic n–π* absorption of butanedione, for example, was almost completely lost within several seconds of addition of H_2O_2 but recovered after the H_2O_2 concentration decreased to below that of the butanedione. Formation of acetic acid by competitive oxidative decomposition of butanedione was confirmed by ^{13}C NMR spectroscopy and constituted an important side reaction. The formation of peracetic acid was excluded under the reaction conditions employed, because peracetic acid does not react directly with electron-deficient alkenes.[168]

The formation of pyridine-2-carboxylic acid from polypyridyl ligands in itself is of only secondary importance; i.e., as a route to catalyst deactivation. However, although it is a very unlikely combination of conditions (i.e., the presence of a ketone solvent with acetate), the catalytic system obtained from the ligand degradation products is highly active in the oxidation of alkenes. This is perhaps an extreme example of a general challenge facing mechanistic studies – the identification of the catalyst, resting state and active species, actually engaging in the catalysis observed.

4.1.2. Manganese tmtacn Based Oxidation Catalysts

As discussed above, the discovery of the catalytic activity of complexes based on the ligand 1,4,7-trimethyl-1,4,7-triazacyclononane (tmtacn), by Hage et al.[106] in the mid-1990s, prompted interest in the capability of these complexes to engage the productive use of H_2O_2 in oxidation and bleaching catalysis. The application of manganese complexes of tacn ligands in oxidation catalysis was reviewed recently by Saisaha et al.[5] and by Watkinson et al.,[6,170] and hence only aspects with regard to the coordination and redox chemistry of the complexes and mechanisms will be discussed in this section.

Several studies in the late 1990s demonstrated that the catalytic activity of **18** increased with respect to catalytic

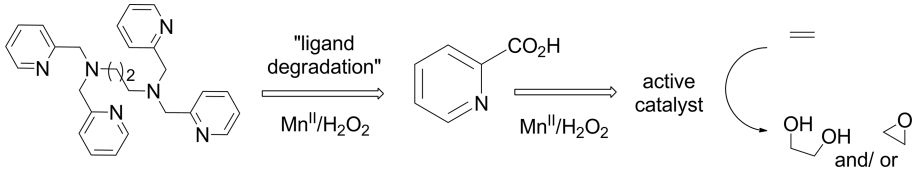

Scheme 7. Oxidative decomposition of polypyridyl ligands to pyridine-2-carboxylic acid (PCA), which was found to be the ligand responsible for the manganese-based oxidation catalysis observed with H_2O_2 and alkenes.[166]

oxidative transformations (such as alkene epoxidation) in the presence of certain additives, together with suppression of the disproportionation of H_2O_2.[112–117] de Vos et al. demonstrated that efficient epoxidation of a wide range of alkenes with decreased H_2O_2 decomposition could be achieved by addition of carboxylic acids such as fumaric acid or the use of an oxalate buffered solution.[171] Shortly after, Berkessel and Sklorz[114] noted that addition of L-ascorbic acid and sodium ascorbate was also effective in both regards. Shul'pin and co-workers demonstrated that the addition of a large excess of acetic acid (with respect to substrate) was effective in promoting the C–H oxygenation activity of **18**.[40,172]

More recently, attention has focused on understanding the mechanism by which **18** catalyses reactions and, in particular, the role played by the various additives that were reported to enhance catalytic efficiency.[5,92,117,119] de Boer et al. showed that carboxylic acids served multiple roles in facilitating the oxidation of alkenes by **18**; that is, to protonate **18** and thereby shift its reduction potential positively to allow reduction, to suppress disproportionation of H_2O_2, to act as a ligand in, for example, **9a** and to stabilise the complex under the reaction conditions. Notably, a substantial lag period prior to the onset of substrate conversion was observed in reactions with **18** in which H_2O_2 was added continuously.[92] The results of UV/Vis absorption spectroscopic analysis confirmed that at the end of the lag period a sudden conversion of **18** into the bis-μ-carboxylato bridged complex **9a** occurred concomitant with the onset of alkene oxidation. Although the precise pathway for conversion of **18** into **9a** is still unclear,[173] cyclic voltammetry and spectroelectrochemistry confirmed that the reduction of **18** by H_2O_2 is required prior to protonation (by a carboxylic acid) of the complex and that, upon reduction, a rapid cascade of reactions led ultimately to near quantitative conversion of **18** into **9a** (see above). The assignment of **9a** as a resting state of the catalyst was confirmed by the absence of a lag period when it was used as catalyst in place of **18**.

4.1.3. Role of Carboxylic Acids in Catalysis with 9a

Identifying the role the carboxylic acid plays as a ligand was key to understanding the effect that variation in the carboxylic acids had on both reactivity (increasing with an increase in the electron deficiency of the carboxylato ligand) and selectivity with respect to epoxidation/*cis*-dihydroxylation (with preference for the *cis*-diol product increasing with the steric bulk of the 2,6-position of benzoic acids).[117]

A key question remained, however, as to the nature of the species that engages in oxygen transfer to the substrate. Regardless of its specific structure, with the exception of oxalic acid,[119] the conversion of alkenes into both *cis*-diol and epoxide products began simultaneously at the end of the lag period, which suggested that a common active species is responsible for both *cis*-dihydroxylation and epoxidation.[92] Furthermore, the oxidation activity of **18** (with CCl_3CO_2H) observed in solvents other than acetonitrile, e.g., acetone, *t*BuOH/H_2O and tetrahydrofuran (THF), correlated to the stability of **9a** in those solvents; that is, the less stable **9a** was found to be, the shorter the time for which reactivity was observed. A further point is that complex **9a** was found to be relatively stable in the presence of H_2O_2, whereas the related complexes **9b**–**c** underwent conversion into **9a** upon addition of H_2O_2. It is apparent therefore that **9a** is either a resting state in the cycle, with its reaction with H_2O_2 being the rate-limiting step, or it is a reservoir for the catalytically active species. Direct oxygen transfer from **9a** was also excluded. The later observation that moderate (up to 54%) enantioselectivity in *cis*-dihydroxylation could be achieved by using chiral carboxylic acids confirmed that the form of the catalyst engaged in oxygen transfer bears at least one carboxylato ligand.[174]

Although, mononuclear high-valent species are frequently proposed as the active species in regard to oxygen transfer to substrate, the data available support the involvement of dinuclear structures that are similar to **9a**. The model most consistent with the experimental data available

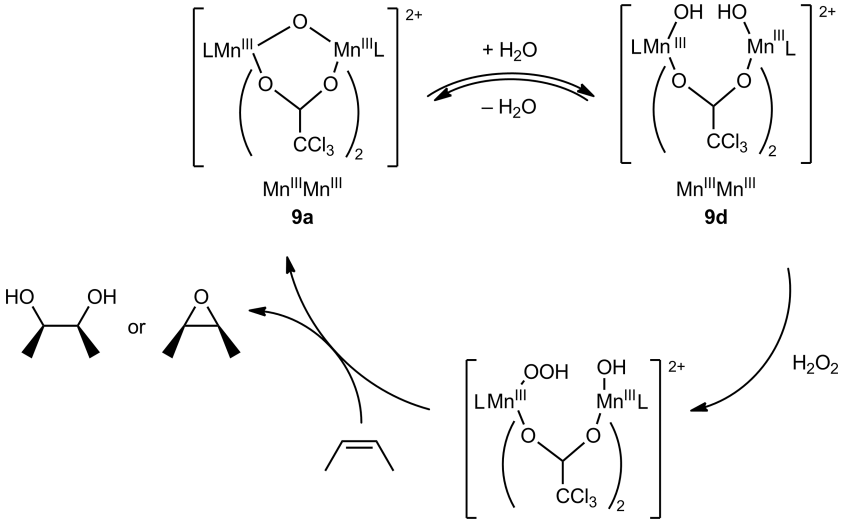

Scheme 8. Proposed catalytic cycle for **9a** in the oxidation of alkenes.[92]

is one in which a $Mn^{III}(O–OH)Mn^{III}(OH)$ species is formed by reaction of **9a** or **9d** with H_2O_2 (Scheme 8). Such a first step is consistent with an associative mechanism for the exchange of the μ-oxido bridge with $H_2{}^{18}O$ (see above) and is consistent with the increased rate of $H_2{}^{18}O$ exchange and catalytic activity observed with electron-deficient carboxylates such as μ-$CCl_3CO_2^-$. The presence of Mn^{III}–OH proximal to the Mn^{III}–O–OH bond would be expected to polarise the O–O bond, allowing for hetereolytic rather than homolytic cleavage. For the *cis*-diol product, one oxygen originated from H_2O_2 and one from H_2O as shown by ^{18}O labelling studies. In contrast, for the epoxide, oxygen incorporation from both H_2O_2 as well as from H_2O was observed, the ratio being dependent upon the μ-carboxylate bridging ligand, with increased electron-withdrawing character favouring incorporation of oxygen from water.

4.1.4. Catalysis with 9a and Other Additives

In contrast, several mechanistic studies on Mn-tmtacn catalysts have led to mono or dinuclear high-valent oxidising species being proposed.[175] Lindsay-Smith and coworkers studied the oxidation of a range of phenolic substrates and azo dyes by **18** in the presence and the absence of H_2O_2 in basic aqueous solution. A catalytically active mononuclear manganese species was proposed based on kinetic and EPR studies.[176–178]

The oxidation of phenols and epoxidation of cinnamic acid by a combination of tmtacn ligand and Mn^{II} salt was studied by ESI-MS from which high-valent Mn^{IV}=O and Mn^{V}=O species were proposed.[177] Of particular interest was the effect of additives (and potential co-ligands) on the rate of conversion observed by loss in UV/Vis absorption of the cinnamic acid at 260 nm and by ESI-MS, by following the disappearance of the signal at *m*/*z* 147 (cinnamate) and formation of a new signal at *m*/*z* 163 (epoxide product) in negative ion mode. In the absence of additives, two signals appeared at *m*/*z* 277 and 259 in positive ion mode, which were assigned to the mononuclear Mn^{IV} ions $[Mn^{IV}(tmtacn)(OH)_3]^+$ (**42**) and $[Mn^{IV}(tmtacn)(O)(OH)_2]^+$ (**43**), respectively (Figure 12).

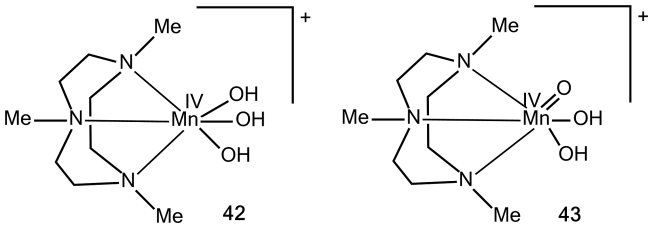

Figure 12. Complexes **42** and **43** proposed to be the active catalysts in the oxidation of phenolics and cinnamates.[177]

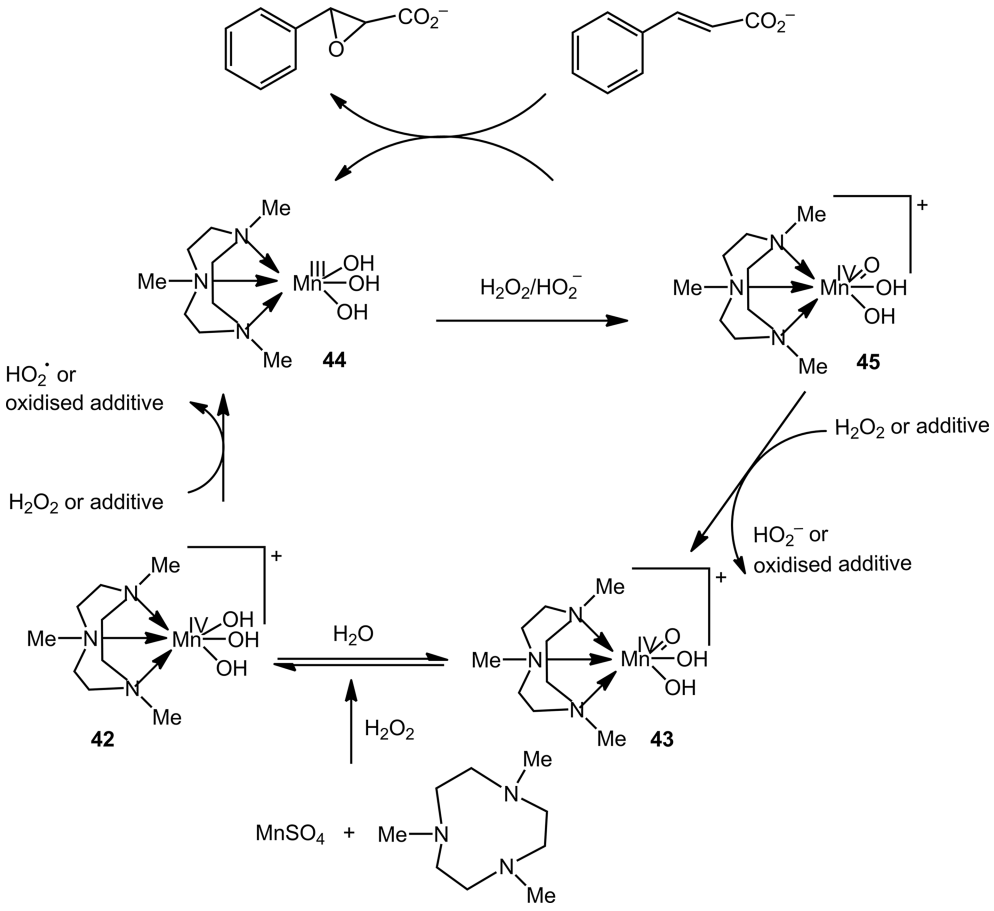

Scheme 9. Mechanisms proposed for the oxidation of cinnamates by Mn-tmtacn complexes proposed by Gilbert, Lyndsay-Smith and coworkers.[176–178]

ESI-MS studies did not yield evidence for the formation of manganese complexes with various additives; that is, such complexes are either not formed or decomposed during MS analysis or were ESI-MS silent. The presence of peracids or manganese hydroperoxide complexes, such as those proposed by Busch and co-workers[159] for related aza-ligand based complexes (see above), was excluded because a longer lag phase and a lower rate of epoxidation was observed with peracetic acid. Analogy with Mn^{III} salens and tetraarylporphyrins led to the proposal that Mn^{V}=O species was the epoxidising agent, and ^{18}O-labelling experiments confirmed H_2O_2 as the source of oxygen in the product. Compounds **42** and **43**, which were detected by ESI-MS,[177] form from a mixture of $Mn^{II}SO_4$, tmtacn and H_2O_2, and undergo one-electron reduction by either H_2O_2 or an additive, to an ESI-MS-silent Mn^{III} complex (**44**; Scheme 9). Subsequent oxidation with H_2O_2 could yield $[Mn^{V}(tmtacn)(O)(OH)_2]^+$ (**45**), which, in turn, was proposed to be the species responsible for the epoxidation of cinnamate.

Watkinson et al.[179] reported recently a study of the initial rates of epoxidation of styrene derivatives by H_2O_2 with a number of Mn-tmtacn catalysts and chiral BINOL-based additives. It was noted that the method used to prepare the catalysts is likely to influence the mechanistic pathway followed. Indeed, this point can possibly be made more general, when one considers the earlier study by de Boer et al.[119] in which oxalic acid and ascorbic acid with **18** were compared with other carboxylic acids as additives. In that study it was found that, for oxalic acid, a switch in the active species (and product distribution) was observed after several hours of reaction, concomitant with the appearance of species similar to **9a**.

4.1.5. Mn-Me$_4$dtne Based Oxidation Catalysts

Although structurally analogous to the tridentate tmtacn based manganese complexes discussed above, the complex $[Mn^{III}Mn^{IV}(\mu\text{-}O)_2(\mu\text{-}CH_3COO)(Me_4dtne)](PF_6)_2$ {**46**, where Me_4dtne = 1,2-bis(4,7-dimethyl-1,4,7-triazacyclonon-1-yl)ethane} (Figure 13), reported first by Wieghardt and co-workers,[180] behaves differently with respect to the relative propensity towards dissociation and exchange of the μ-acetato and μ-O ligand. The pH dependence of the coordination chemistry of this complex was reported recently by Abdolahzadeh et al.[181] in relation to its application in the oxidation of flavones, as models for natural dyes, by H_2O_2 in water. The pH dependence of the structure of the complex present in water between pH 6 and 11 and the dissociation and association of the carboxylato ligands that are commonly used as additives under bleaching conditions was investigated with UV/Vis absorption, Raman and EPR spectroscopy, as well as with cyclic voltammetry.

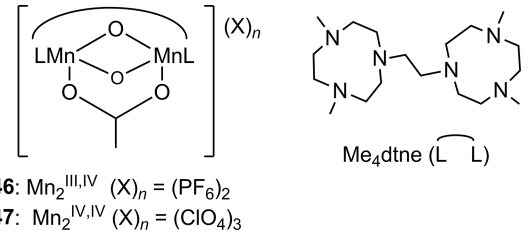

Figure 13. Structure of complexes **46** and **47** and the ligand Me_4dtne.

The changes observed (i.e., the shift in redox potential and blueshift in absorbance) upon an increase in pH from 6 to 11, were assigned to dissociation of the μ-acetato ligand (Figure 14). This was confirmed by partial recovery of the original spectral features and the return of the redox wave of **46** at higher potential upon addition of excess acetate at high pH. Notably, addition of carbonate resulted in similar recovery in the absorption spectrum but not the redox chemistry due to formation of **51** (Scheme 10).

The 16-line EPR spectrum of **46** (g = 2) showed a change in the hyperfine coupling constants going from aMn = 70 G

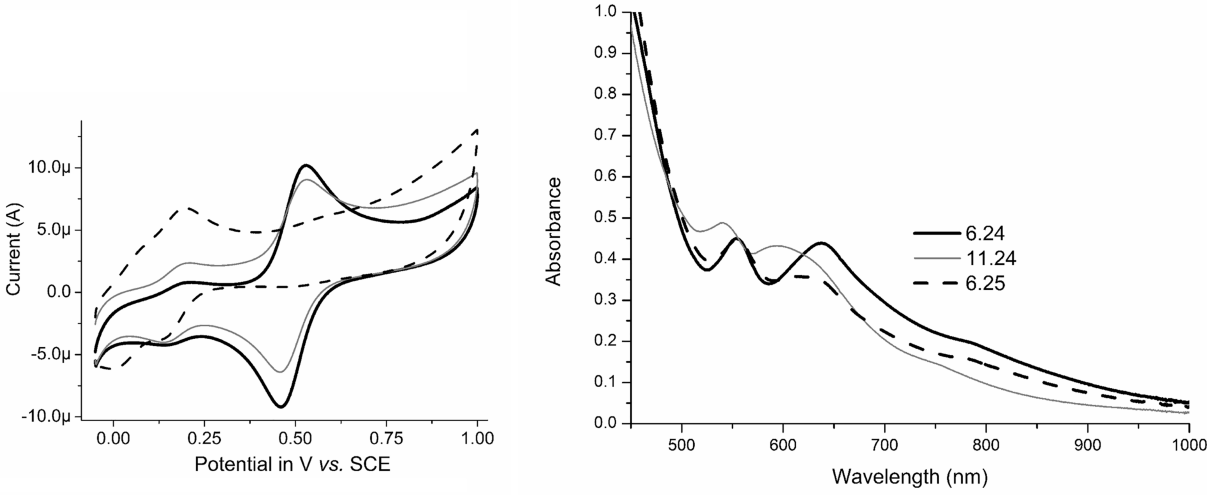

Figure 14. (left) Cyclic voltammetry of **46** (1 mM) in 0.1 M KNO_3 (aq) at a GC electrode at pH 6 (black), pH 8 (grey) and pH 11 (dashed). Sweep rate: 100 mV s^{-1}. (right) UV/Vis absorption spectra of **46** (1 mM) in water at, initially, pH 6.24, then pH 11.24 and finally pH 6.25. Reproduced from ref.[181] with permission. Copyright the Royal Society of Chemistry (2014).

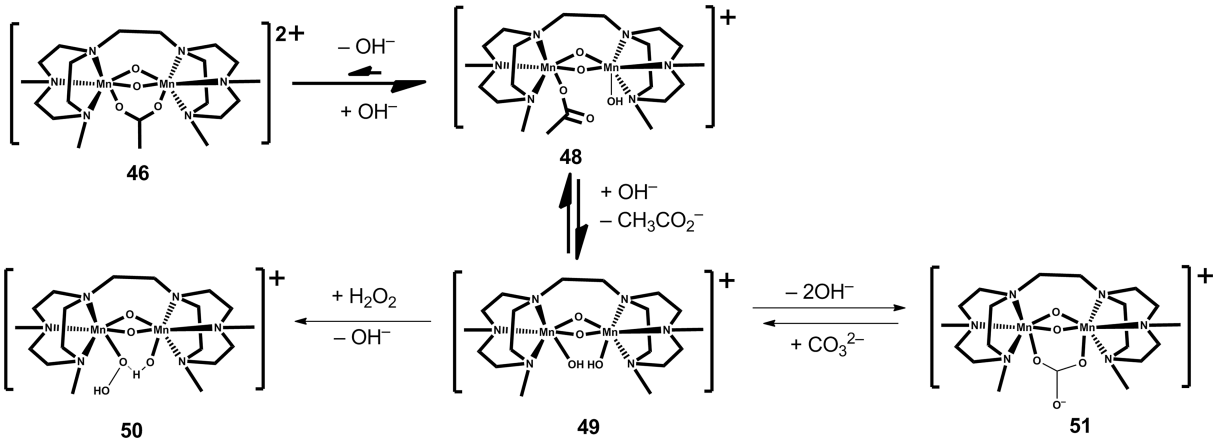

Scheme 10. Equilibrium between **46** and the acetate dissociated forms **48** and **49** present at high pH and possible structure of hydroperoxy intermediate **50** formed at high pH.[181]

at both pH 6 and pH 8 to 76 G at pH 11.[181] This change indicated that a minor change in coordination had occurred, with either monodentate acetate (**48**) or complete acetate dissociation (**49**) occurring. Notably, the $Mn^{IV}Mn^{IV}$ analogue **47** was found to be unstable above pH 7, i.e., in the pH range relevant to catalytic oxidations, converting quantitatively into **46** even in the presence of H_2O_2. The thermodynamic stability of the μ-oxido bridge and the key role that the dissociation of the carboxylato ligand plays in achieving activity in the $Mn^{III}Mn^{IV}$ oxidation state in aqueous solution is consistent with observations by Cooper et al. for manganese complexes with bipyridine and phenanthroline ligands.[80]

These observations indicated that at high pH (>10), partial dissociation of the acetato ligand provided complex **48** and/or **49** (Scheme 10). This behaviour, together with higher activity of **46** above pH 10, suggested that the opening of the μ-carboxylate bridge provides exchangeable coordination sites in the complex that can interact with H_2O_2 and enables the complex to act as a catalyst in the bleaching of substrates. Hence, the addition of carboxylates such as carbonate (either added deliberately or present due to absorption of CO_2 from the atmosphere) or sequestrants such as diethylene triamine pentaacetic acid (DTPA) can block vacant coordination sites of **49** inhibiting the reaction with H_2O_2 and thus decreasing catalytic activity. Hence, the optimisation of the concentrations of such additives should be taken into consideration in bleaching processes to improve the catalytic activity of **46**.

The behaviour of **46** is in contrast to that observed by de Boer et al. for the structurally analogous $[Mn^{III}Mn^{III}(\mu\text{-}O)(\mu\text{-}RCO_2)_2(tmtacn)_2]^{2+}$ complexes, for which loss of the μ-carboxylato ligand resulted in loss of catalytic activity (see above).[92] Indeed, comparison of these two classes of complexes, which have similar structures with both μ-oxido and μ-carboxylato bridges, highlights the conclusion that small changes in ligand structure can have a profound effect on whether it is the oxido or carboxylato bridges that open and provide the free coordination site necessary to react with H_2O_2.

4.2. Manganese-Catalysed Oxidation of Dyes in Aqueous Media (Bleaching)

Beyond the selective oxidations of organic substrates, the catalysed bleaching of bulk materials such as laundry, raw cotton and wood pulp are key industrial processes.[182–184] Despite appearing diverse, the chromophores that need to be bleached in these bulk processes tend to be similar, and are predominantly polyphenolic substances. In contrast to fine chemical processes, the goal is primarily bleaching either by oxidation of the chromophores so that they lose visible absorbance or by increasing their water solubility sufficiently to allow their removal from the substrates.[183] Primarily for economic reasons, the oxidants used in these processes are either chlorine based, H_2O_2, ozone and/or peracetic acid; however, environmental concerns have favoured the increasing use of chlorine-free oxidants in recent years. The relatively low reactivity of H_2O_2 requires, however, the use of either high temperatures and basic conditions or the use of catalysts, including those based on manganese.[185,186]

Eldik and co-workers[187] have studied the ability of manganese catalysts to activate H_2O_2 to oxidise various azo and phenolic dyes in carbonate buffers (Scheme 11).

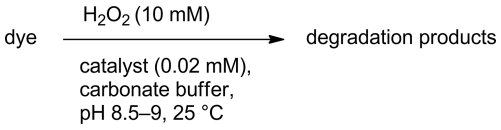

Scheme 11. Conditions used in catalytic dye oxidation with manganese catalysts by Eldik and co-workers.[187]

The dyes examined generally showed $n\rightarrow\pi^*$ absorptions between 375–490 nm, depending on the substituents present, the pK_a values of the dyes and pH.

The structure of the manganese complexes present at pH 8.5 depends on the concentration of hydrogen carbonate. The broad absorption at 300 nm, which appears upon addition of HCO_3^- to $Mn^{II}(aq)$, which increased with carbonate concentration. The formation of the Mn^{II}-HCO_3^- complex proceeded with first-order kinetics (k_{obs})

prior to precipitation of $Mn^{II}CO_3$ in the absence of oxidisable substrates.

Coordination of hydrogen carbonate to Mn^{II} resulted in a shift in the oxidation potential from 0.52 to 0.48 V (vs. Ag/AgCl). In the presence of the azo and polyphenolic dyes, precipitation of manganese carbonate was not observed even at high concentrations of carbonate due to complexation between the dyes and manganese, which was manifested in changes to the UV/Vis absorption spectrum of the dye and a shift to less positive potentials of the first oxidation. Complexation energies for a series of different Mn–dye complexes, as calculated by DFT methods, indicated stabilisation of the Mn^{II} ion by hydroxyl-containing ligands compared with nitrogen-donor ligands. The activity towards dye bleaching was increased by the presence of a hydroxyl group in the dyes. The formation of high-valent manganese oxido intermediates upon reaction of Mn^{II} with H_2O_2 in hydrogen carbonate solution was confirmed by UV/Vis absorption spectroscopy, which was manifested in the appearance of a broad band at 460 nm. Furthermore, the six-line ESR signal at g ≈ 2, characteristic of Mn^{II} in an octahedral environment, which was broadened upon addition of hydrogen carbonate, was replaced by a broad signal at g ≈ 4, which is characteristic of a high-spin Mn^{IV} species. In the absence of stabilising ligands, the catalytically inactive species $Mn^{IV}O_2$ is formed instead. The formation of radicals was excluded by the use of a radical scavenger, *t*BuOH, by EPR and UV/Vis spectroscopy, and the absence of evidence for Mn^{III} ions is consistent with the assumption that Mn^{II} and Mn^{IV} are the main species present during oxidation catalysis.

Kinetic analysis indicated that two equivalents of HCO_3^- were required for catalysed oxidation, with one equivalent needed for the formation of a complex with the Mn^{II} ion and a second equivalent required for the formation of peroxocarbonate in situ. Peroxocarbonate is a more reactive oxidising agent than H_2O_2 itself, which was attributed to carbonate being a better leaving group compared with hydroxide. Maximum bleaching activity was observed between pH 8.2 and 8.5. At higher pH, a decrease in the rate of the reaction was observed, which was ascribed to deprotonation of the $HOOCO_2^-$ to form the less electrophilic oxidant CO_4^{2-}; at still higher pH, the spontaneous decomposition of H_2O_2 and precipitation of the MnO_2 was observed.

The formation of peroxocarbonate in situ was assigned as the rate-limiting step in the reaction, with the Mn^{IV}=O intermediate formed upon reaction of hydroperoxycarbonate reacting with the dye substrates rapidly to regenerate the Mn^{II} species (Scheme 12).

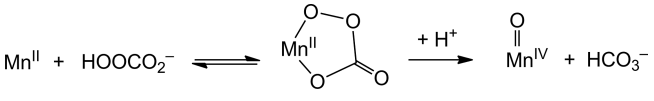

Scheme 12. Formation of a Mn^{IV}-oxido complex from the reaction of Mn^{II} with percarbonate formed in situ.

The catalytic activity of Mn^{II} ions towards bleaching of dyes was compared[188] with the catalytic activity of both $[Mn^{II}(bpy)_2Cl_2]$ and $[Mn^{III}Mn^{IV}(\mu\text{-}O)_2(bpy)_4](ClO_4)_3 \cdot 2H_2O$. Both complexes showed maximum reactivity at ca. pH 8.7. The effect of carbonate concentration on the observed rate of oxidation was also similar for both catalysts, indicating a common reactive intermediate. Indeed, in the absence of carbonate, in CHES (N-cyclohexyl-2-aminoethanesulfonic acid) buffer, catalytic activity was negligible. Moreover, it was shown that monocarboxylate ions such as acetate, hydrogen carbonate and formate, enhanced the activity of the catalyst towards olefin epoxidation with H_2O_2 whereas dicarboxylate ions, such as oxalate, resulted in lower reactivity. EPR spectroscopy in aqueous hydrogen carbonate showed that for both $[Mn^{II}(bpy)_2Cl_2]$ and $[Mn^{III}Mn^{IV}(\mu\text{-}O)_2(bpy)_4](ClO_4)_3 \cdot 2H_2O$, a broad, weak signal at g = 4–5 was observed, which was attributed to a mononuclear Mn^{IV} species, in addition to a six-line signal at g = 2, characteristic of an octahedral mononuclear Mn^{II} complex upon addition of H_2O_2. No evidence for the presence of mixed-valent oxido-bridged manganese complexes or for radical species was obtained in the presence of either catalyst.

The key step was proposed to be a two-electron oxidation of a monomeric Mn^{II} precursor to a Mn^{IV}=O species, manifested in the appearance of an absorption band at 450 nm, assigned to a LMCT transition, upon addition of H_2O_2 for both catalysts. The authors concluded that ligand displacement by hydrogen carbonate was not occurring in this system.

5. Conclusion

The central role that manganese-based enzymes play in the control of reactive oxygen species and, of course, in the OEC of PSII has driven the design and synthesis of a wide range of manganese complexes both as structural models and as functional mimics. These efforts have been stimulated further by the high activity that can be achieved with manganese catalysts in the selective oxidation of organic substrates. In contrast to iron complexes based on similar ligands, manganese-based systems show a remarkable propensity to form well-defined multinuclear complexes with oxido and carboxylato bridging ligands. The activity of these catalysts, and the activity of the enzymes that have inspired their preparation, is critically dependent on the redox state and on redox-driven changes in coordination mode. The clearest example being carboxylate shifts and opening of oxido bridges. It is apparent, however, that although general trends are observed, i.e., that an increase in oxidation state favours oxido over carboxylato ligands and hence drives ligand exchange, even with relatively similar ligands, two complexes can show different propensities to exchange oxido or carboxylato ligands to provide free coordination sites for binding to reactive oxygen species such as H_2O_2. From the perspective of oxidation catalysis, the variation in coordination chemistry seen with multinuclear manganese complexes poses considerable challenges to understanding both the nature of the species that engage in

oxygenation of substrates and, especially, the key role played by additives in overall reaction mechanisms. Of course, such challenges are fertile ground for the discovery of new reactivity and for pushing the limits of our ability to develop highly active catalysts and to study highly complex systems.

Acknowlwdgments

Financial support comes from the European Research Council (ERC-2011-StG-279549, to W. R. B.), the Netherlands Fund for Technology and Science STW (11059, to S. A., J. W. d. B, W. R. B.), and the Ministry of Education, Culture and Science (Gravity program 024.001.035, to W. R. B.). COST action CM1003 "Biological Oxidation Reactions – Mechanism and Design of New Catalysts" is acknowledged for discussion.

[1] S. J. Lippard, J. M. Berg, *Principles of Bioinorganic Chemistry*, University Science Books, Mill Valley, California, **1994**.
[2] M. Hudlicky, *Oxidations in Organic Chemistry*, ACS, Washington, DC, **1990**.
[3] R. A. Sheldon, J. K. Kochi, *Metal-Catalyzed Oxidations of Organic Compounds: Mechanistic Principles and Synthetic Methodology Including Biochemical Processes*, Academic Press, New York, NY, USA, **1981**.
[4] E. M. McGarrigle, D. G. Gilheany, *Chem. Rev.* **2005**, *105*, 1563–1602.
[5] P. Saisaha, J. W. de Boer, W. R. Browne, *Chem. Soc. Rev.* **2013**, *42*, 2059–2074.
[6] K. F. Sibbons, K. Shastri, M. Watkinson, *Dalton Trans.* **2006**, 645–661.
[7] a) J. E. Backvall, *Modern Oxidation Methods*, Wiley-VCH, Weinheim, Germany, 2nd ed. **2010**; b) B. Meunier, *Chem. Rev.* **1992**, *92*, 1411–1456.
[8] R. Hage, J. W. de Boer, F. Gaulard, K. Maaijen, *Adv. Inorg. Chem.* **2013**, *65*, 85–116.
[9] J. M. Campos-Martin, G. Blanco-Brieva, J. L. G. Fierro, *Angew. Chem. Int. Ed.* **2006**, *45*, 6962–6984; *Angew. Chem.* **2006**, *118*, 7116.
[10] J. P. Klinman, *J. Biol. Inorg. Chem.* **2001**, *6*, 1–13.
[11] N. Lane, *Oxygen, the Molecule that Made the World*, Oxford University Press, Oxford, UK, **2002**.
[12] C. W. Cady, R. H. Crabtree, G. W. Brudvig, *Coord. Chem. Rev.* **2008**, *252*, 444–445.
[13] B. Loll, J. Kern, W. Saenger, A. Zouni, J. Biesiadka, *Nature* **2005**, *438*, 1040–1044.
[14] J. Yano, J. Kern, K. Sauer, M. J. Latimer, Y. Pushkar, J. Biesiadka, B. Loll, W. Saenger, J. Messinger, A. Zouni, V. K. Yachandra, *Science* **2006**, *314*, 821–825.
[15] W. Lubitz, E. J. Reijerse, J. Messinger, *Energy Environ. Sci.* **2008**, *1*, 15–31.
[16] J. Barber, *Chem. Soc. Rev.* **2009**, *38*, 185–196.
[17] K. Kawakami, N. Kamiya, J. R. Shen, *J. Photochem. Photobiol. B: Biology* **2011**, *104*, 9–18.
[18] Y. Umena, K. Kawakami, J. R. Shen, N. Kamiya, *Nature* **2011**, *473*, 55–60.
[19] V. V. Barynin, M. M. Whittaker, S. V. Antonyuk, V. S. Lamzin, P. M. Harrison, P. J. Artymiuk, J. W. Whittaker, *Structure* **2001**, *9*, 725–738.
[20] J. W. de Boer, W. R. Browne, B. L. Feringa, R. Hage, *C. R. Chim.* **2007**, *10*, 341–354.
[21] D. W. Christianson, *Prog. Biophys. Mol. Biol.* **1997**, *67*, 217–252.
[22] G. N. Landis, J. Tower, *Mech. Ageing Dev.* **2005**, *126*, 365–379.
[23] O. Iranzo, *Bioorg. Chem.* **2011**, *39*, 73–87.
[24] D. W. Christianson, *Acc. Chem. Res.* **2005**, *38*, 191–201.
[25] S. Mukhopadhyay, S. K. Mandal, S. Bhaduri, W. H. Armstrong, *Chem. Rev.* **2004**, *104*, 3981–4026.
[26] A. J. Wu, J. E. Penner-Hahn, V. L. Pecoraro, *Chem. Rev.* **2004**, *104*, 903–938.
[27] C. Herrero, B. Lassallekaiser, W. Leibl, A. Rutherford, A. Aukauloo, *Coord. Chem. Rev.* **2008**, *252*, 456–458.
[28] M. Collomb, A. Deronzier, *Eur. J. Inorg. Chem.* **2009**, 2025–2046.
[29] M. Wiechen, H. M. Berends, P. Kurz, *Dalton Trans.* **2012**, *41*, 21–31.
[30] I. Ojima, *Catalytic Asymmetric Synthesis* VCH Publishers, New York, **1993**.
[31] J. T. Groves, M. K. Stern, *J. Am. Chem. Soc.* **1987**, *109*, 3812–3814.
[32] J. Limburg, J. S. Vrettos, H. Chen, J. C. de Paula, R. H. Crabtree, G. W. Brudvig, *J. Am. Chem. Soc.* **2001**, *123*, 423–430.
[33] D. H. R. Barton, S. Y. Choi, B. Hu, J. A. Smith, *Tetrahedron* **1998**, *54*, 3367–3378.
[34] R. Tagore, H. Chen, R. H. Crabtree, G. W. Brudvig, *J. Am. Chem. Soc.* **2006**, *128*, 9457–9465.
[35] G. Yin, M. Buchalova, A. M. Danby, C. M. Perkins, D. Kitko, J. D. Carter, W. M. Scheper, D. H. Busch, *Inorg. Chem.* **2006**, *45*, 3467–3474.
[36] A. Murphy, T. D. P. Stack, *J. Mol. Catal. A* **2006**, *251*, 78–88.
[37] W. Adam, K. J. Roschmann, C. R. Saha-Moller, D. Seebach, *J. Am. Chem. Soc.* **2002**, *124*, 5068–5073.
[38] N. S. Finney, P. J. Pospisil, S. Chang, M. Palucki, R. G. Konsler, K. B. Hansen, E. N. Jacobsen, *Angew. Chem. Int. Ed. Engl.* **1997**, *36*, 1720–1723; *Angew. Chem.* **1997**, *109*, 1798.
[39] A. Murphy, G. Dubois, T. D. P. Stack, *J. Am. Chem. Soc.* **2003**, *125*, 5250–5251.
[40] G. B. Shul'pin, G. Süss-Fink, J. R. L. Smith, *Tetrahedron* **1999**, *55*, 5345–5385.
[41] A. Murphy, A. Pace, T. D. P. Stack, *Org. Lett.* **2004**, *6*, 3119–3122.
[42] I. Garcia-Bosch, A. Company, X. Fontrodona, X. Ribas, M. Costas, *Org. Lett.* **2008**, *10*, 2095–2098.
[43] K. Nakamoto, *Infrared and Raman Spectra of Inorganic and Coordination Compounds*, 3rd ed., Wiley, New York, **1978**.
[44] Y. Sufferen, F. G. Rollet, C. Reber, *Comments Inorg. Chem.* **2011**, *32*, 246–276.
[45] W. R. Browne, J. J. McGarvey, *Coord. Chem. Rev.* **2007**, *251*, 454–473.
[46] J. J. McGarvey, A. Draksharapu, W. R. Browne, *Spectroscopy, photophysics and structural dynamics in metal-centred species, some recent investigations: from spin-crossover complexes and oxygen activation to photocatalysis*, in: *Spectroscopic Properties of Inorganic and Organometallic Compounds: Techniques, Materials Applications* (Eds.: J. Yarwood, R. Douthwaite, S. Duckett), RSC Publishing, Cambridge, UK, **2013**, vol. 44, 68–94.
[47] J. I. Zink, K.-S. K. Shin, *Molecular Distortions in Excited Electronic States Determined from Electronic and Resonance Raman Spectroscopy*, in: *Advances in Photochemistry* (Eds.: D. H. Volman, G. S. Hammond, D. C. Neckers), John Wiley & Sons, Inc., Hoboken, NJ, USA, **1991**, vol. 16, 119–214.
[48] K. S. K. Shin, J. I. Zink, *Inorg. Chem.* **1989**, *28*, 4358–4366.
[49] L. Tutt, J. I. Zink, *J. Am. Chem. Soc.* **1986**, *108*, 5830–5836.
[50] G. R. Eaton, S. S. Eaton, *Comprehensive Coordination Chemistry II* (Eds.: J. A. McCleverty, T. J. Meyer), Elsevier, Amsterdam, **2004**.
[51] D. P. Goldberg, J. Telser, J. Krzystek, A. G. Montalban, L. C. Brunel, A. G. M. Barrett, B. M. Hoffman, *J. Am. Chem. Soc.* **1997**, *119*, 8722–8723.
[52] A. K. Brisdon, *Inorganic Spectroscopic Methods*, Oxford University Press, Oxford, UK, **1998**, p. 57–73.
[53] R. Hage, B. Krijnen, J. B. Warnaar, F. Hartl, D. J. Stufkens, T. L. Snoeck, *Inorg. Chem.* **1995**, *34*, 4973–4978.

[54] M. C. Feiters, W. Meyer-Klaucke, *Practical approaches to biological inorganic chemistry* (Eds.: R. R. Crichton, R. O. Louro), Elsevier, Oxford, UK, **2013**, chapter 6.
[55] H. Dau, A. Grundmeier, P. Loja, M. Haumann, *Phil. Trans. R. Soc. B* **2008**, *363*, 1237–1244.
[56] A. J. Bard, L. R. Faulkner, *Electrochemical Methods, Fundamentals and Applications*, John Wiley & Sons, New York, **1980**.
[57] R. Parsons, *Chem. Rev.* **1990**, *90*, 813–826.
[58] D. T. Sawyer, A. Sobkowiak, J. L. Roberts Jr., *Electrochemistry for Chemists*, John Wiley & Sons, New York, **1995**.
[59] W. R. Heineman, *J. Chem. Educ.* **1983**, *60*, 305–308.
[60] W. Kaim, A. Klein (Eds.), *Spectroelectrochemistry*, Royal Society of Chemistry, Cambridge, UK, **2008**.
[61] O. Bortolini, V. Conte, *Mass Spectrom. Rev.* **2006**, *25*, 724–740.
[62] R. Colton, A. D'Agostino, J. C. Traeger, *Mass Spectrom. Rev.* **1995**, *14*, 79–106.
[63] V. Kertesz, G. J. Van Berkel, *Electroanalysis* **2001**, *13*, 1425–1430.
[64] F. Zhou, G. J. Van Berkel, *Anal. Chem.* **1995**, *67*, 3643–3649.
[65] C. F. Bokman, C. Zettersten, P. J. R. Sjoberg, L. Nyholm, *Anal. Chem.* **2004**, *76*, 2017–2024.
[66] I. Prat, J. S. Mathieson, M. Güell, X. Ribas, J. M. Luis, L. Cronin, M. Costas, *Nature Chem.* **2011**, *3*, 788–793.
[67] R. J. Debus, *Coord. Chem. Rev.* **2008**, *252*, 244–258.
[68] I. A. Abreu, D. E. Cabelli, *Biochim. Biophys. Acta Proteins Proteomics* **2010**, *1804*, 263–274.
[69] G. C. Dismukes, *Chem. Rev.* **1996**, *96*, 2909–2906.
[70] K. N. Ferreira, T. M. Iverson, K. Maghlaoui, J. Barber, S. Iwata, *Science* **2004**, *303*, 1831–1838.
[71] A. W. Rutherford, A. Boussac, *Science* **2004**, *303*, 1782–1784.
[72] M. Suga, F. Akita, K. Hirata, G. Ueno, H. Murakami, Y. Nakajima, T. Shimizu, K. Yamashita, M. Yamamoto, H. Ago, J. R. Shen, *Nature* **2015**, *517*, 99–103.
[73] B. Kok, B. Forbush, M. McGloin, *Photochem. Photobiol.* **1970**, *11*, 457–475.
[74] H. Dau, M. Haumann, *Biochim. Biophys. Acta Bioenerg.* **2007**, *1767*, 472–483.
[75] K. J. Young, Y. Gao, G. W. Brudvig, *Aust. J. Chem.* **2011**, *64*, 1221–1228.
[76] J. Limburg, J. S. Vrettos, L. M. Liable-Sands, A. L. Rheingold, R. H. Crabtree, G. W. Brudvig, *Science* **1999**, *283*, 1524–1527.
[77] a) M. Yagi, A. Syouji, S. Yamada, M. Komi, H. Yamazaki, S. Tajima, *Photochem. Photobiol. Sci.* **2009**, *8*, 139–147; b) H. Yamazaki, A. Shouji, M. Kajita, M. Yagi, *Coord. Chem. Rev.* **2010**, *254*, 2483–2491; c) M. Yagi, K. Narita, *J. Am. Chem. Soc.* **2004**, *126*, 8084–8085; d) K. Narita, T. Kuwabara, K. Sone, K. Shimizu, M. Yagi, *J. Phys. Chem. B* **2006**, *110*, 23107–23114; e) A. K. Poulsen, A. Rompel, C. J. McKenzie, *Angew. Chem. Int. Ed.* **2005**, *44*, 6916–6920; *Angew. Chem.* **2005**, *117*, 7076; f) Y. Naruta, M. Sasayama, T. Sasaki, *Angew. Chem. Int. Ed. Engl.* **1994**, *33*, 1839–1841; *Angew. Chem.* **1994**, *106*, 1964; g) Y. Shimazaki, T. Nagano, H. Takesue, B. Ye, F. Tani, Y. Naruta, *Angew. Chem. Int. Ed.* **2004**, *43*, 98–100; *Angew. Chem.* **2004**, *116*, 100; h) W. Ruettinger, M. Yagi, K. Wolf, S. Bernasek, G. C. Dismukes, *J. Am. Chem. Soc.* **2000**, *122*, 10353–10357; i) M. Yagi, K. V. Wolf, P. J. Baesjou, S. L. Bernasek, G. C. Dismukes, *Angew. Chem. Int. Ed.* **2001**, *40*, 2925–2928; *Angew. Chem.* **2001**, *113*, 3009; j) R. Brimblecombe, A. Koo, G. C. Dismukes, G. F. Swiegers, L. Spiccia, *J. Am. Chem. Soc.* **2010**, *132*, 2892–2894.
[78] a) R. Manchanda, G. W. Brudvig, R. H. Crabtree, *Coord. Chem. Rev.* **1995**, *144*, 1–38; b) T. G. Carrell, A. M. Tyryshkin, G. C. Dismukes, *J. Biol. Inorg. Chem.* **2002**, *7*, 2–22; c) V. K. Yachandra, K. Sauer, M. P. Klein, *Chem. Rev.* **1996**, *96*, 2927–2950; d) C. S. Mullins, V. L. Pecoraro, *Coord. Chem. Rev.* **2008**, *252*, 416–443.
[79] M. Watkinson, A. Whiting, C. A. McAuliffe, *J. Chem. Soc., Chem. Commun.* **1994**, *18*, 2141–2142.
[80] S. R. Cooper, M. Calvin, *J. Am. Chem. Soc.* **1977**, *99*, 6623–6630.
[81] P. M. Kelley, S. Izawa, *Biochim. Biophys. Acta* **1978**, *502*, 198–201.
[82] J. Sinclair, *Biochim. Biophys. Acta* **1984**, *764*, 247–252.
[83] P. O. Sandusky, C. F. Yocum, *Biochim. Biophys. Acta* **1986**, *849*, 85–93.
[84] D. J. MacLachlan, J. H. A. Nugent, J. T. Warden, M. C. W. Evans, *Biochim. Biophys. Acta* **1994**, *1188*, 325–334.
[85] H. Kuhne, V. A. Szalai, G. W. Brudvig, *Biochemistry* **1999**, *38*, 6604–6613.
[86] R. Tagore, R. H. Crabtree, G. W. Brudvig, *Inorg. Chem.* **2007**, *46*, 2193–2203.
[87] M. Lundberg, M. R. A. Blomberg, P. E. M. Siegbahn, *Theor. Chem. Acc.* **2003**, *110*, 130–143.
[88] a) W. H. Casey, B. L. Phillips, *Geochim. Cosmochim. Acta* **2001**, *65*, 705–714; b) A. P. Lee, B. L. Phillips, W. H. Casey, *Geochim. Cosmochim. Acta* **2002**, *66*, 577–587.
[89] H. Chen, J. W. Faller, R. H. Crabtree, G. W. Brudvig, *J. Am. Chem. Soc.* **2004**, *126*, 7345–7349.
[90] a) H. H. Thorp, J. E. Sarneski, G. W. Brudvig, R. H. Crabtree, *J. Am. Chem. Soc.* **1989**, *111*, 9249–9250; b) J. E. Sarneski, H. H. Thorp, G. W. Brudvig, R. H. Crabtree, G. K. Schulte, *J. Am. Chem. Soc.* **1990**, *112*, 7255–7260; c) R. Manchanda, G. W. Brudvig, R. H. Crabtree, *New J. Chem.* **1994**, *18*, 561–568.
[91] a) J. Messinger, M. Badger, T. Wydrzynski, *Proc. Natl. Acad. Sci. USA* **1995**, *92*, 3209–3213; b) W. Hillier, J. Messinger, T. Wydrzynski, *Biochemistry* **1998**, *37*, 16908–16914; c) W. Hillier, T. Wydrzynski, *Biochemistry* **2000**, *39*, 4399–4405; d) G. Hendry, T. Wydrzynski, *Biochemistry* **2002**, *41*, 13328–13334; e) G. Hendry, T. Wydrzynski, *Biochemistry* **2003**, *42*, 6209–6217; f) W. Hillier, T. Wydrzynski, *Phys. Chem. Chem. Phys.* **2004**, *6*, 4882–4889.
[92] J. W. de Boer, W. R. Browne, J. Brinksma, P. L. Alsters, R. Hage, B. L. Feringa, *Inorg. Chem.* **2007**, *46*, 6353–6372.
[93] G. Berggren, M. F. Anderlund, S. Styring, A. Thapper, *Inorg. Chem.* **2012**, *51*, 2332–2337.
[94] G. Berggren, A. Thapper, P. Huang, L. Eriksson, S. Styring, M. F. Anderlund, *Inorg. Chem.* **2011**, *50*, 3425–3430.
[95] K. Wieghardt, U. Bossek, D. Ventur, J. Weiss, *J. Chem. Soc., Chem. Commun.* **1985**, 347–349.
[96] K. Wieghardt, U. Bossek, B. Nuber, J. Weiss, J. Bonvoisin, M. Corbella, S. E. Vitols, J. J. Girerd, *J. Am. Chem. Soc.* **1988**, *110*, 7398–7411.
[97] P. Kurz, M. F. Anderlund, N. Shaikh, S. Styring, P. Huang, *Eur. J. Inorg. Chem.* **2008**, 762–770.
[98] R. Lomoth, P. Huang, J. T. Zheng, L. C. Sun, L. Hammarström, B. Åkermark, S. Styring, *Eur. J. Inorg. Chem.* **2002**, 2965–2974.
[99] Y. Nishida, M. Nasu, *Inorg. Chim. Acta* **1991**, *190*, 1–3.
[100] L. Dubois, R. Caspar, L. Jacquamet, P. E. Petit, M. F. Charlot, C. Baffert, M. N. Collomb, A. Deronzier, J. M. Latour, *Inorg. Chem.* **2003**, *42*, 4817–4827.
[101] G. Eilers, C. Zettersten, L. Nyholm, L. Hammarström, R. Lomoth, *Dalton Trans.* **2005**, 1033–1041.
[102] It should be noted that although the presence of ligand-exchange products, in: neat acetonitrile was confirmed by ESI-MS, this was ascribed to the presence of adventitious water.
[103] M. F. Anderlund, J. Högblom, W. Shi, P. Huang, L. Eriksson, H. Weihe, S. Styring, B. Åkermark, R. Lomoth, A. Magnuson, *Eur. J. Inorg. Chem.* **2006**, 5033–5047.
[104] P. Huang, A. Magnuson, R. Lomoth, M. Abrahamsson, M. Tamm, L. Sun, B. van Rotterdam, J. Park, L. Hammarström, B. Åkermark, S. Styring, *J. Inorg. Biochem.* **2002**, *91*, 159–172.
[105] P. Chaudhuri, K. Wieghardt, *Prog. Inorg. Chem.* **1987**, *35*, 329–436.
[106] R. Hage, J. E. Iburg, J. Kerschner, J. H. Koek, E. L. M. Lempers, R. J. Martens, U. S. Racherla, S. W. Russell, T. Swarthoff, M. R. P. Van Vliet, J. B. Warnaar, L. Van Der Wolf, B. Krijnen, *Nature* **1994**, *369*, 637–639.

[107] A. Niemann, U. Bossek, K. Wieghardt, C. Butzlaff, A. X. Trautwein, B. Nuber, *Angew. Chem. Int. Ed. Engl.* **1992**, *31*, 311–313; *Angew. Chem.* **1992**, *104*, 345.
[108] H. H. Thorp, G. W. Brudwig, *New J. Chem.* **1991**, *15*, 479–490.
[109] V. L. Pecoraro, *Manganese Redox Enzymes*, VCH: New York, **1992**.
[110] V. L. Pecoraro, M. J. Baldwin, A. Gelasco, *Chem. Rev.* **1994**, *94*, 807–826.
[111] K. Wieghardt, *Angew. Chem. Int. Ed. Engl.* **1989**, *28*, 1153–1172; *Angew. Chem.* **1989**, *101*, 1179.
[112] D. E. De Vos, T. Bein, *J. Organomet. Chem.* **1996**, *520*, 195–200.
[113] D. E. De Vos, T. Bein, *Chem. Commun.* **1996**, 917–918.
[114] A. Berkessel, C. A. Sklorz, *Tetrahedron Lett.* **1999**, *40*, 7965–7968.
[115] J. Brinksma, L. Schmieder, G. Van Vliet, R. Boaron, R. Hage, D. E. De Vos, P. L. Alsters, B. L. Feringa, *Tetrahedron Lett.* **2002**, *43*, 2619–2622.
[116] a) C. B. Woitiski, Y. N. Kozlov, D. Mandelli, G. V. Nizova, U. Schuchardt, G. B. Shul'pin, *J. Mol. Catal. A* **2004**, *222*, 103–119; b) B. Liu, Y. Chen, C.-Z. Yu, Z. W. Shen, *Chin. J. Chem.* **2003**, *21*, 833–838; c) J. Y. Ryu, S. O. Kim, W. Nam, S. Heo, J. Kim, *Bull. Korean Chem. Soc.* **2003**, *24*, 1835–1837.
[117] J. W. de Boer, J. Brinksma, W. R. Browne, A. Meetsma, P. L. Alsters, R. Hage, B. L. Feringa, *J. Am. Chem. Soc.* **2005**, *127*, 7990–7991.
[118] P. Saisaha, L. Buettner, M. van der Meer, R. Hage, B. L. Feringa, W. R. Browne, J. W. de Boer, *Adv. Synth. Catal.* **2013**, *355*, 2591–2603.
[119] J. W. de Boer, P. L. Alsters, A. Meetsma, R. Hage, W. R. Browne, B. L. Feringa, *Dalton Trans.* **2008**, 6283.6295.
[120] Y. Kono, I. Fridovich, *J. Biol. Chem.* **1983**, *258*, 6015–6019.
[121] V. V. Barynin, A. I. Grebenko, *Dokl. Akad. Nauk SSSR* **1986**, *286*, 461–464.
[122] G. S. Allgood, J. J. Perry, *J. Bacteriol.* **1986**, *168*, 563–567.
[123] T. Amo, H. Atomi, T. Imanaka, *J. Bacteriol.* **2002**, *184*, 3305–3312.
[124] S. V. Antonyuk, W. R. Melik-Adamyan, A. N. Popov, V. S. Lamzin, P. D. Hempstead, P. M. Harrison, P. J. Artymiuk, V. V. Barynin, *Crystallogr. Rep.* **2000**, *45*, 105–116.
[125] V. V. Barynin, P. D. Hempstead, A. A. Vagin, S. V. Antonyuk, W. R. Melik-Adamyan, V. S. Lamzin, P. M. Harrison, P. J. Artymiuk, *J. Inorg. Biochem.* **1997**, *67*, 196.
[126] P. J. Pessiki, S. V. Khangulov, D. M. Ho, G. C. Dismukes, *J. Am. Chem. Soc.* **1994**, *116*, 891–897.
[127] Y. Nishida, T. Akamatsu, K. Tsuchiya, M. Sakamoto, *Polyhedron* **1994**, *13*, 2251–2254.
[128] S. Signorella, C. Hureau, *Coord. Chem. Rev.* **2012**, *256*, 1229–1245.
[129] V. L. Pecoraro, A. Gelasco, M. Baldwin, *Modeling the Chemistry and Properties of Multinuclear Manganese Enzymes* (Ed.: D. P. Kessissoglou), Kluwer Academic Publishers, Dordrecht, The Netherlands, **1995**.
[130] A. Gelasco, V. L. Pecoraro, *J. Am. Chem. Soc.* **1993**, *115*, 7928–7929.
[131] A. Gelasco, M. L. Kirk, J. W. Kampf, V. L. Pecoraro, *Inorg. Chem.* **1997**, *36*, 1829–1837.
[132] J. E. Penner-Hahn, *Structural Properties of the Mn Site in the Mn Catalases* (Ed.: V. L. Pecoraro), VCH Publishers, New York, **1992**, p. 29.
[133] G. S. Waldo, S. Yu, J. E. Penner-Hahn, *J. Am. Chem. Soc.* **1992**, *114*, 5869–5870.
[134] M. Shank, V. V. Barynin, G. C. Dismukes, *Biochemistry* **1994**, *33*, 15433–15436.
[135] E. J. Larson, V. L. Pecoraro, *J. Am. Chem. Soc.* **1991**, *113*, 3810–3818.
[136] S. Signorella, A. Rompel, K. Buldt-Karentzopoulos, B. Krebs, V. L. Pecoraro, J.-P. Tuchagues, *Inorg. Chem.* **2007**, *46*, 10864–10868.
[137] A. E. M. Boelrijk, G. C. Dismukes, *Inorg. Chem.* **2000**, *39*, 3020–3028.
[138] a) A. Gelasco, S. Bensiek, V. L. Pecoraro, *Inorg. Chem.* **1998**, *37*, 3301–3309; b) P. Mathur, M. Crowder, G. Dismukes, *J. Am. Chem. Soc.* **1987**, *109*, 5227–5233; c) P. J. Pessiki, G. C. Dismukes, *J. Am. Chem. Soc.* **1994**, *116*, 898–903; d) Y. Sasaki, T. Akamatsu, K. Tsuchiya, S. Ohba, M. Sakamoto, Y. Nishida, *Polyhedron* **1998**, *17*, 235–242.
[139] a) J. D. Rush, Z. Maskos, *Inorg. Chem.* **1990**, *29*, 897–905; b) C. Philouze, G. Blondin, S. Menage, N. Auger, J.-J. Girerd, D. Vigner, M. Lance, M. Nierlich, *Angew. Chem. Int. Ed. Engl.* **1992**, *31*, 1629–1631; *Angew. Chem.* **1992**, *104*, 1634.
[140] A. E. M. Boelrijk, S. V. Khangulov, G. C. Dismukes, *Inorg. Chem.* **2000**, *39*, 3009–3019.
[141] J. E. Sheats, R. S. Czernuziewicz, G. C. Dismukes, A. L. Rheingold, V. Petrouleas, J. Stubbe, W. H. Armstrong, R. Beer, S. J. Lippard, *J. Am. Chem. Soc.* **1987**, *109*, 1435–1444.
[142] G. B. Deacon, R. J. Phillips, *Coord. Chem. Rev.* **1980**, *33*, 227–250.
[143] C. Palopoli, N. Bruzzo, C. Hureau, S. Ladeira, D. Murgida, S. Signorella, *Inorg. Chem.* **2011**, *50*, 8973–8983.
[144] M. Corbella, G. Fernández, P. González, M. Maestro, M. Font-Bardia, H. Stoeckli-Evans, *Eur. J. Inorg. Chem.* **2012**, 2203–2212.
[145] L. Dubois, J. Pécaut, M. F. Charlot, C. Baffert, M. N. Collomb, A. Deronzier, J. M. Latour, *Chem. Eur. J.* **2008**, *14*, 3013–3025.
[146] T. Katsuki, K. B. Sharpless, *J. Am. Chem. Soc.* **1980**, *102*, 5974–5976.
[147] a) R. C. Michaelson, R. E. Palermo, K. B. Sharpless, *J. Am. Chem. Soc.* **1977**, *99*, 1990–1992; b) C. Bolm, *Coord. Chem. Rev.* **2003**, *237*, 245–256.
[148] a) W. A. Herrmann, R. W. Fischer, M. U. Rauch, W. Scherer, *J. Mol. Catal.* **1994**, *86*, 243–266; b) W. Adam, C. M. Mitchell, *Angew. Chem. Int. Ed. Engl.* **1996**, *35*, 533–535; *Angew. Chem.* **1996**, *108*, 578; c) *Modern Oxidation Methods* (Ed.: J. E. Bäckvall), Wiley-VCH, Weinheim, Germany, **2004**, chapter 2.
[149] a) K. Sato, M. Aoki, M. Ogawa, T. Hashimoto, R. Noyori, *J. Org. Chem.* **1996**, *61*, 8310–8311; b) R. Noyori, M. Aokib, K. Satoc, *Chem. Commun.* **2003**, 1977–1986; c) F. J. Iborra, D. A. Jackson, P. R. Cook, *Science* **2001**, *293*, 1139–1142.
[150] J. M. Garrison, T. C. Bruice, *J. Am. Chem. Soc.* **1989**, *111*, 191–198.
[151] J. P. Collman, A. S. Chien, T. A. Eberspacher, J. I. Brauman, *J. Am. Chem. Soc.* **2000**, *122*, 11098–11100.
[152] F. M. MacDonnell, N. L. P. Fackler, C. Stern, T. V. O'Halloran, *J. Am. Chem. Soc.* **1994**, *116*, 7431–7432.
[153] B. S. Mandimutsira, B. Ramdhanie, R. C. Todd, H. Wang, A. A. Zareba, R. S. Czernuszewicz, D. P. Goldberg, *J. Am. Chem. Soc.* **2002**, *124*, 15170–15171.
[154] S. H. Wang, B. S. Mandimutsira, R. C. Todd, B. Ramdhanie, J. P. Fox, D. P. Goldberg, *J. Am. Chem. Soc.* **2004**, *126*, 18–19.
[155] J. Bernadou, A. Fabiano, A. Robert, B. Meunier, *J. Am. Chem. Soc.* **1994**, *116*, 9375–9376.
[156] J. T. Groves, J. Lee, S. S. Marla, *J. Am. Chem. Soc.* **1997**, *119*, 6269–6273.
[157] a) J. P. Renaud, P. Battioni, J. F. Bartoli, D. Mansuy, *J. Chem. Soc., Chem. Commun.* **1985**, 888–889; b) S. Banfi, F. Legramandi, F. Montanari, G. Pozzi, S. Quici, *J. Chem. Soc., Chem. Commun.* **1991**, 1285–1287.
[158] a) K. Srinivasan, P. Michaud, J. K. Kochi, *J. Am. Chem. Soc.* **1986**, *108*, 2309–2320; b) W. Zhang, J. L. Loebach, S. R. Wilson, E. N. Jacobsen, *J. Am. Chem. Soc.* **1990**, *112*, 2801–2803; c) R. Irie, K. Noda, Y. Ito, N. Matsumoto, T. Katsuki, *Tetrahedron Lett.* **1990**, *31*, 7345–7348.
[159] T. J. Hubin, J. M. McCormick, S. R. Collinson, M. Buchalova, C. M. Perkins, N. W. Alcock, P. K. Kahol, A. Raghunathan, D. H. Busch, *J. Am. Chem. Soc.* **2000**, *122*, 2512–2522.

[160] G. Yin, M. Buchalova, A. M. Danby, C. M. Perkins, D. Kitko, J. D. Carter, W. M. Scheper, D. H. Busch, *J. Am. Chem. Soc.* **2005**, *127*, 17170–17171.
[161] A. Haras, T. Ziegler, *Can. J. Chem.* **2009**, *87*, 33–38.
[162] a) J. Brinksma, R. Hage, J. Kerschner, B. L. Feringa, *Chem. Commun.* **2000**, 537–538; b) J. Brinksma, M. T. Rispens, R. Hage, B. L. Feringa, *Inorg. Chim. Acta* **2002**, *337*, 75–82.
[163] S. Groni, P. Dorlet, G. Blain, S. Bourcier, R. Guillot, E. Anxolabéhère-Mallart, *Inorg. Chem.* **2008**, *47*, 3166–3172.
[164] M. R. Bukowski, S. Zhu, K. D. Koehntop, W. W. Brennessel, L. Que, *J. Biol. Inorg. Chem.* **2004**, *9*, 39–48.
[165] M. Grau, A. Kyriacou, F. C. Martinez, I. M. de Wispelaere, A. J. P. White, G. J. P. Britovsek, *Dalton Trans.* **2014**, *43*, 17108–17119.
[166] D. Pijper, P. Saisaha, J. W. de Boer, R. Hoen, C. Smit, A. Meetsma, R. Hage, R. P. van Summeren, P. L. Alsters, B. L. Feringa, W. R. Browne, *Dalton Trans.* **2010**, *39*, 10375–10381.
[167] P. Saisaha, D. Pijper, J. W. de Boer, R. Hoen, R. P. van Summeren, P. L. Alsters, R. Hage, B. L. Feringa, W. R. Browne, *Org. Biomol. Chem.* **2010**, *8*, 4444–4450.
[168] J. Dong, P. Saisaha, T. G. Meinds, P. L. Alsters, E. G. Ijpeij, R. P. van Summeren, B. Mao, M. Fañanás-Mastral, J. W. de Boer, R. Hage, B. L. Feringa, W. R. Browne, *ACS Catal.* **2012**, *2*, 1087–1096.
[169] J. Dong, D. Unjaroen, F. Meccozi, E. C. Harvey, P. Saisaha, D. Pijper, J. W. de Boer, P. Alsters, B. L. Feringa, W. R. Browne, *ChemSusChem* **2013**, *6*, 1774–1778.
[170] G. De Faveri, G. Ilyashenko, M. Watkinson, *Chem. Soc. Rev.* **2011**, *40*, 1722–1760.
[171] D. E. De Vos, B. F. Sels, M. Reynaers, Y. V. S. Rao, P. A. Jacobs, *Tetrahedron Lett.* **1998**, *39*, 3221–3224.
[172] G. B. Shul'pin, G. Suss-Fink, L. S. Shul'pina, *J. Mol. Catal. A* **2001**, *170*, 17–34.
[173] This process has been studied in detail recently: D. Angelone, S. Abdolahzadeh, J. W. de Boer, W. R. Browne, *Eur. J. Inorg. Chem.* **2015**, DOI: 10.1002/ejic.201500195.
[174] J. W. de Boer, W. R. Browne, S. R. Harutyunyan, L. Bini, T. D. Tiemersma-Wegman, P. L. Alsters, R. Hage, B. L. Feringa, *Chem. Commun.* **2008**, *32*, 3747–3749.
[175] R. Hage, A. Lienke, *J. Mol. Catal. A* **2006**, *251*, 150–158.
[176] a) B. C. Gilbert, N. W. J. Kamp, J. R. Lindsay-Smith, J. Oakes, *J. Chem. Soc. Perkin Trans. 2* **1997**, 2161–2166; b) B. C. Gilbert, N. W. J. Kamp, J. R. Lindsay-Smith, J. Oakes, *J. Chem. Soc. Perkin Trans. 2* **1998**, 1841–1844.
[177] B. C. Gilbert, J. R. Lindsay-Smith, M. S. Newton, J. Oakes, R. Pons i Prats, *Org. Biomol. Chem.* **2003**, *1*, 1568–1577.
[178] J. R. Lindsay-Smith, B. C. Gilbert, A. Mairata i Payeras, J. Murray, T. R. Lowdon, J. Oakes, R. Pons i Prats, P. H. Walton, *J. Mol. Catal. A* **2006**, *251*, 114–122.
[179] G. Ilyashenko, G. De Faveri, S. Masoudi, R. Al-Safadi, M. Watkinson, *Org. Biomol. Chem.* **2013**, *11*, 1942–1951.
[180] T. Weyhermüller, K. Wieghardt, *J. Inorg. Biochem.* **1991**, *43*, 371.
[181] S. Abdolahzadeh, N. M. Boyle, M. L. Hoogendijk, R. Hage, J. W. de Boer, W. R. Browne, *Dalton Trans.* **2014**, *43*, 6322–6332.
[182] R. Hage, J. W. de Boer, F. Gaulard, K. Maaijen, *Adv. Inorg. Chem.* **2013**, *65*, 85–116.
[183] R. Hage, A. Lienke, *Angew. Chem. Int. Ed.* **2006**, *45*, 206–222.
[184] R. Hage, A. Lienke, *J. Mol. Catal. A* **2006**, *251*, 150–158.
[185] a) D. E. Richardson, H. Yao, K. M. Frank, D. A. Bennett, *J. Am. Chem. Soc.* **2000**, *122*, 1729–1739; b) H. Yao, D. E. Richardson, *J. Am. Chem. Soc.* **2000**, *122*, 3220–3221.
[186] B. S. Lane, K. Burgess, *J. Am. Chem. Soc.* **2001**, *123*, 2933–2934.
[187] S. Rothbart, R. van Eldik, *Adv. Inorg. Chem.* **2013**, *65*, 165–216, and references cited therein.
[188] S. Rothbart, E. Ember, R. van Eldik, *Dalton Trans.* **2010**, *39*, 3264–3272.

Received: February 6, 2015
Published Online: June 30, 2015

